Spatial and temporal variations of the concentrations of PM_{10}, $PM_{2.5}$ and PM_1 in China

Y. Q. Wang[1*], X. Y. Zhang[1*], J. Y. Sun[1], X. C. Zhang[2], H. Z. Che[1], Y. Li[1]

[1]{Laboratory of Atmospheric Chemistry, Chinese Academy of Meteorological Sciences, Beijing, China}

[2]{Meteorological Observation Center, Beijing, China}

Correspondence to: Y. Q. Wang (wangyq@cams.cma.gov.cn) , X. Y. Zhang (xiaoye@cams.cma.gov.cn)

Abstract:

Concentrations of PM_{10}, $PM_{2.5}$ and PM_1 were monitored at 24 CAWNET (China Atmosphere Watch Network) stations from 2006 to 2014. The highest particulate matter (PM) concentrations were observed at the stations of Xian, Zhengzhou and Gucheng, on the Guanzhong Plain and the Hua Bei Plain (HBP). The second highest PM concentrations were observed in northeast China, followed by southern China. According to the latest air quality standards of China, 14 stations reached the PM_{10} standard, and only 7 stations, mainly rural and remote stations, reached the $PM_{2.5}$ standard. The ratios of $PM_{2.5}$ to PM_{10} showed a clear increasing trend from northern to southern China, because of the substantial contribution of coarse mineral aerosol in northern China. The ratios of PM_1 to $PM_{2.5}$ were higher than 80% at most stations. PM concentrations tended to be highest in winter and lowest in summer at most stations, and mineral dust influenced the results in spring. A decreasing interannual trend was observed on the HBP and in southern China for the period 2006 to 2014, but an increasing trend occurred at some stations in northeast China. Bimodal and unimodal diurnal variation patterns were identified at urban stations. Both emissions and meteorological variations dominate the long-term PM concentration trend, while meteorological factors play a leading role in the short-term.

Keywords: particulate matter, observation, spatiotemporal variation

1. Introduction

Tropospheric aerosols are important because of their strong influence on the climate system through both direct and indirect effects. These include the direct effect of scattering and absorbing radiant energy, and the indirect effect of modifying the microphysical properties of clouds, and hence their radiative properties and lifetime (Haywood and Boucher, 2000). They also attract attention because of their adverse effects on visibility (Watson, 2002) and human health (Delfino et al., 2005; Pope III and Dockery, 2006). Therefore, the spatial and temporal variation of aerosols is essential to understand, but remains a complex subject because of their ephemeral nature and the complexity of their physical and chemical properties (Ramanathan et al., 2001).

Particle size is considered a key parameter to define the impact of particulate matter (PM) on human health; specifically, fine PM ($PM_{2.5}$ and PM_1) poses a greater health risk than coarse PM (PM_{10}) (Oberdörster et al., 2005). There have been numerous network-based observation studies of the $PM_{2.5}$ concentration and chemical composition in North America and Europe. For example, based on a dataset across 19 Canadian sites, most of the $PM_{2.5}$ concentrations were found to be below 26 μg m^{-3}, and $PM_{2.5}$ accounted for 49% of the measured PM_{10} (Brook et al., 1997). Meanwhile, Eldred et al. (1997) reported that $PM_{2.5}$ and PM_{10} particulate concentrations measured at 42 sites of the Interagency Monitoring of Protected Visual Environments (IMPROVE) network over the 1993 seasonal year (March 1993 to February 1994) showed the $PM_{2.5}$ concentration had a large gradient from west to east in the US, averaging 3 μg m^{-3} in most of the west compared with 13 μg m^{-3} in the Appalachian region. Another study, based on 143 IMPROVE sites in the year 2001, showed that sulfates, carbon and crustal material were responsible for most of the measured $PM_{2.5}$ at the majority of sites in the US (Malm et al., 2004). The temporal variation and spatial distribution of $PM_{2.5}$ concentrations have also been reported in Switzerland (Gehrig and Buchmann, 2003), Austria (Gomiscek et al., 2004), and six central and eastern European countries (Houthuijs et al., 2001).

As a country with a rapidly developing economy, China has suffered from a serious air pollution problem in recent years due to substantial increases in energy consumption and other related production of large amounts of aerosols and precursor gas emissions (Zhang et al., 2009). At the coarse end of the spectrum (PM_{10}), the spatial distribution and interannual variation of concentrations has been comprehensively studied using a dataset accumulated from 86 Chinese cites (Qu et al., 2010). Furthermore, the chemical compositions of PM_{10} samples were investigated at 16 sites over China, and the result indicated a dominant scattering feature of aerosols (Zhang et al., 2012). Network-based studies of $PM_{2.5}$ observations have, however, been limited to certain seasons in a single year (Cao et al., 2012), and most other research has focused on one or more of the largest cities (He et al., 2001; Wang et al., 2002; Wang et al., 2006; Wei et al., 1999; Yao et al., 2002; Zhao et al., 2009; Zheng et al., 2005). The focus on $PM_{2.5}$ needs to improve, not least because the growing problem of heavy haze has compelled the Chinese government to pay greater attention to $PM_{2.5}$ monitoring and air quality standards. Indeed, the Ministry of Environmental Protection of China issued new ambient air quality standards in 2012, among which the $PM_{2.5}$ concentration was the first to be included. Subsequently, the construction of a network of national environmental $PM_{2.5}$ monitoring stations began in 2013.

In this paper, we present a long-term PM_{10}, $PM_{2.5}$ and PM_1 monitoring dataset from 2006 to 2014, based on 24 stations of CAWNET (China Atmosphere Watch Network), operated by the China Meteorological Administration (CMA). The spatial pattern of average PM concentration levels and the relationships among them are reported. In addition, their seasonal and interannual variations are presented.

2. The near real-time PM dataset

The PM_{10}, $PM_{2.5}$ and PM_1 concentrations were monitored at 24 CAWNET stations from 2006 to 2014 using GRIMM dust monitor EDM 180 instruments with 31 different size channels at a flow rate of 1.2 L/min. The instrument is designed to measure the particle size distribution and particulate mass, based on a light scattering measurement of individual particles in the sampled air. GRIMM-developed protocols were used to convert the measured size number distribution to a mass concentration consistent with U.S. Environmental Protection Agency protocols for measuring PM using the aerodynamic diameter. A Nafion dryer was equipped at the inlet to exclude fine particulate water, but the nonvolatile and semi-volatile components are included in the measurement result (Grimm and Eatough, 2009). The instruments were calibrated annually using a calibration tower that permitted powder injection (on demand) of aerosol particles in a wide size range of 0.2–30 μm. The operation was fully computer-controlled and permitted access to one to three spectrometers in comparison to one reference "mother unit". The 5-min averaged PM_{10}, $PM_{2.5}$ and PM_1 concentrations were recorded at each station and transported to the CMA information center hourly in near real-time.

The PM concentration results from the GRIMM instruments were compared to those from tapered element oscillating microbalance (TEOM) instruments reported in a number of other studies (Grimm and Eatough, 2009; Hansen et al., 2010). The instruments were in good agreement; linear regression with TEOM data from Rubidoux (California, USA) yielded a slope of 1.10 ± 0.05, with an intercept of −3.9 ± 4.2 μg m^{-3} and an uncertainty of 9.9% (Grimm and Eatough, 2009). Furthermore, GRIMM and TEOM measurements in Beijing have shown a close linear relationship, suggesting that optical measurements can be used to derive $PM_{2.5}$ and account for semi-volatile material in aerosols (Sciare et al., 2007; Zhao et al., 2011).

The 24 PM observation stations are detailed in Table 1, and a map of their distribution is given in Figure 1. Most of the stations were located in East China, an area of high population density and rapid economic development, meaning the PM emitted from human activities was mainly recorded. The stations were classified as urban/suburban, rural and remote stations, according to their location. Unlike rural stations, remote stations were located in areas far away from regions of strong anthropogenic emissions, and thus natural emissions and long-range transport of anthropogenic air pollution were the main sources of PM at these stations.

3. Results and discussion

3.1. Average PM_{10}, $PM_{2.5}$ and PM_1 levels in China

The averaged PM concentration values are presented in Table 2, and their distributions in Figure 1. The highest PM_{10}, $PM_{2.5}$ and PM_1 concentrations were observed at the stations of Xian (135.4, 93.6 and 77.0 μg m^{-3}, respectively), Zhengzhou (131.7, 84.8 and 71.0 μg m^{-3}, respectively) and Gucheng (127.8, 89.7 and 79.4 μg m^{-3}, respectively), which are located in the most polluted areas of the Hua Bei Plain (HBP) and the Guanzhong Plain. Although Gucheng is a rural site, it is located in the rapid urbanization area around Beijing, and is therefore subjected to associated large quantities of air pollutants. These areas were also identified by Zhang et al. (2012) as having experienced similar visibility changes and large visibility loss in the past 40 years. The stations all recorded very high coarse and fine PM concentrations, implying high emissions of both primary emitted mineral particles and secondary anthropogenic particles in these areas. Qingdao is a coastal city with relatively low PM concentrations compared with inland cities on the HBP.

The PM concentrations were also high in northeast China, which is an established industrial area. The ensemble average values of the five urban stations of Ansan, Shenyang, Benxi, Fushun and Shiping were 88.8, 58.4 and 49.8 μg m^{-3}, for PM_{10}, $PM_{2.5}$ and PM_1, respectively. Dandong is a rural station with relatively low PM concentrations.

The similarity among the PM values for Chifeng, Erlianhaote and Yulin is due to their location, far from regions of intensive economic development but strongly affected by sand and dust storms given their proximity to dust source areas. Thus, the average PM_{10} concentrations were much higher than the $PM_{2.5}$ and PM_1 concentrations at these sites. For example, the average PM_{10} concentration at Chifeng, which is surrounded by sandy land, was 88.0 μg m^{-3}, compared with 42.4 and 32.6 μg m^{-3} for $PM_{2.5}$ and PM_1, respectively.

Chengdu, the capital of Sichuan Province, is located in the Sichuan Basin, another highly polluted area. High aerosol optical depth and low visibility, due to the poor dispersion conditions and heavy local industrial emissions, have been reported for this site (Li et al., 2003; Luo et al., 2001; Zhang et al., 2012). In the present study, the average PM_{10}, $PM_{2.5}$ and PM_1 concentrations were 78.0, 59.5 and 52.7 μg m^{-3}, respectively.

There are three stations in the South China area: Panyu, located in Guangzhou City, the capital of Guangdong Province, which is the center of the Pearl River Delta region; Nanning, the capital of Guangxi Province; and Guilin, a famous tourist city, also located in Guangxi Province. The ensemble average PM concentrations of these three sites were 55.8, 43.1 and 38.8 μg m^{-3} for PM_{10}, $PM_{2.5}$ and PM_1, respectively.

Significant visibility loss and relatively high PM_{10} concentrations have been observed over the middle and lower reaches of the Yangtze River after the 1980s due to the rapid economic development that has taken place in this region (Qu et al., 2010; Zhang et al., 2012). Although there was no urban site available for this study to help quantify the high PM concentrations in this region, the background conditions and temporal variance could be determined from the rural site data. Dongtan, near Shanghai City, is located on Chongming Island, where there were low PM concentrations (31.9, 27.4 and 24.8 μg m^{-3} for PM_{10}, $PM_{2.5}$ and PM_1, respectively) due to the substantial influence of clean sea air mass. The ensemble average PM concentrations for Lushan, Changde and Jinsha were 44.3, 37.2 and 33.6 μg m^{-3} for PM_{10}, $PM_{2.5}$ and PM_1, respectively.

Lhasa, the capital of Tibet Autonomous Region, is located in the center of the Tibetan Plateau at a very high altitude of 3663 m. The $PM_{2.5}$ and PM_1 concentrations in Lhasa were low, with average values of 14.0 and 9.6 μg m^{-3}, respectively, because of its relatively small population and few industrial emissions. However, the average PM_{10} concentration was 37.7 μg m^{-3}, mainly due to the high amounts of fugitive dust from dry and bare land and the impacts of regional dust storm events (Chen et al., 2013). As a result, minerals are the main constituent of aerosol samples in this area (Zhang et al., 2012).

The lowest PM concentration values were observed in the two remote sites of Akadala and Shangri-La. The lower altitude and stronger contribution of soil dust at Akadala (Qu et al., 2009), located in a dry region, lead to higher PM concentrations than at the Shangri-La site.

According to the latest air quality standards of China (annual averaged PM_{10} and $PM_{2.5}$ concentrations of 70 and 35 μg m^{-3}), 14 stations reached the PM_{10} standard, while only 7 stations, mainly rural and remote stations, reached the $PM_{2.5}$ standard. The ratio of substandard (daily averaged PM_{10} or $PM_{2.5}$ concentrations that exceed the standard values) days to total observation days at each station was calculated using the standard daily averaged PM_{10} and $PM_{2.5}$ concentrations of 150 and 75 μg m^{-3} (Table 2). Substandard days of PM_{10} and $PM_{2.5}$ represented more than 30% and 50% of the total period at the three most polluted sites (Xian, Zhengzhou and Gucheng). The $PM_{2.5}$ substandard day ratios at five other stations (Chengdu, Anshan, Shenyang, Benxi and Siping) were also larger than 20%.

Average PM_{10}, $PM_{2.5}$ and PM_1 concentrations at urban/suburban stations in this study were 83.6, 56.3 and 48.3 μg m^{-3}, respectively. Meanwhile, the values were 54.8, 36.3 and 30.8 μg m^{-3} at rural stations, and 11.9, 7.5 and 6.1 μg m^{-3} at remote stations. All values were much higher than results from other countries. For example, the observed PM concentration in Canada between 1984 to 1993 showed the average $PM_{2.5}$ concentration was 14.1 and 10.7 μg m^{-3} at urban and rural stations, respectively (Brook et al., 1997). The average $PM_{2.5}$ values from west to east across the IMPROVE network in 1993 (most stations located in rural areas) were 3 to 13 μg m^{-3} (Eldred et al., 1997). Observations in Switzerland from 1998 to 2001 showed average PM_{10} and $PM_{2.5}$ concentrations at urban/suburban stations of 27.7 and 20.1 μg m^{-3}, respectively (Gehrig and Buchmann, 2003). In Austria, in 1998, the annual mean mass concentrations of PM_{10}, $PM_{2.5}$ and PM_1 were around 28, 20 and 16 μg m^{-3}, respectively, at urban sites, and slightly lower at rural sites (Gomiscek et al., 2004). The average PM_{10} and $PM_{2.5}$ concentrations were 23.9 and 16.3 μg m^{-3}, respectively, for the period 2008–2009 in the Netherlands (Janssen et al., 2013). Between October 2008 and April 2011, the 20 study areas of the European ESCAPE project showed

PM_{10} and $PM_{2.5}$ with similar spatial patterns; specifically, low concentrations in Northern Europe and high concentrations in Southern and Eastern Europe (Eeftens et al., 2012). With the rapid urbanization and corresponding increase in traffic and energy consumption in India, the ambient concentrations of fine PM are also high. For example, measurements in New Delhi during August to December 2007 showed concentrations of PM_{10}, $PM_{2.5}$ and PM_1 ranged from 20 to 180 μg m^{-3} during the monsoon season, and from 100 to 500 μg m^{-3} during winter (Tiwari et al., 2012).

3.2. Relationships between PM_{10}, $PM_{2.5}$ and PM_1 concentrations

The squared correlation coefficient (R^2) values of the linear fit between PM_{10} and $PM_{2.5}$ and between PM_1 and $PM_{2.5}$ are given in Table 2. Higher values indicate that the two PM size bins were closer matched in terms of their sources. At most stations, the R^2 values between PM_1 and $PM_{2.5}$ were higher than the values between $PM_{2.5}$ and PM_{10}. This is because PM_1 and $PM_{2.5}$ both belong to fine particle size bins, which are normally emitted from the same sources. For example, the R^2 values were 0.7857 between $PM_{2.5}$ and PM_{10}, and 0.9689 between PM_1 and $PM_{2.5}$, at Gucheng. Correlation analysis is sensitive to outliers, and thus sand storm events may have impacted upon the results considerably, due to abnormally high concentration values. There were four strong dust storm event days at Akdala in 2012, on April 21 and 22, and May 9 and 20, which resulted in the four outliers shown in Figure 2a, and the low R^2 value of 0.5346 between PM_1 and $PM_{2.5}$. The value increased to 0.9406 when the four outliers were removed (Figure 2b). Similar results were also observed at Yulin and Erlianhaote around dust storm source regions (Table 2).

The average values of the daily $PM_{2.5}/PM_{10}$ and $PM_1/PM_{2.5}$ ratios are listed in Table 2. The spatial distribution of the average $PM_{2.5}/PM_{10}$ ratios (Figure 3a) shows lower values in northern China, influenced by Asian sand and dust storms (Wang et al., 2008; Zhang et al., 2003). The values were also influenced by fugitive dust due to the low precipitation amounts in northern China, especially at Lhasa, Erlanhaote, Yulin and Chifeng, with ratios of less than 0.6. The ratios at the stations in northeast China were between 0.6 and 0.7, except at Dandong where the value was 0.71. The values were also low at Zhengzhou and Akdala, at 0.68 and 0.67, respectively. The highest ratio was 0.9 at Dongtan, and the other stations with ratios higher than 0.8 were Chengdu, Changde, Guilin, Jinsha and Lushan. The values were between 0.7 and 0.8 at other stations. The $PM_1/PM_{2.5}$ ratios (Figure 3b) showed a similar spatial distribution, but the values were higher than $PM_{2.5}/PM_{10}$. The lowest ratio of 0.6 was also observed at Lhasa, and the values at most stations in southern China were greater than or equal to 0.9.

3.3. Seasonal variation

The seasonal variations of PM_{10} concentrations (Figure 4a) show that winter and spring were the most polluted seasons at all sites except Lushan, where the highest value was observed in autumn. This result is consistent with a previous study of PM_{10} variation across China from 2000 to 2006 (Qu et al., 2010). The higher winter concentrations were caused by higher emissions during the cold season from heating, and more stagnant weather conditions with a lower planetary boundary layer. The opposite conditions and more precipitation due to the summer monsoon resulted in the lowest PM_{10} concentration values in summer. Spring is the dust storm season in East Asia (Qian et al., 2004; Wang et al., 2008; Zhou and Zhang, 2003), which leads to high PM_{10} concentrations in dust source regions and downwind areas in northern China. For example, the PM_{10} concentrations in spring were much higher than other seasons at the dust source sites of Yulin and Erlianhaote.

For $PM_{2.5}$, winter was still the most polluted season at most sites, while the contribution of spring decreased substantially in northern China (Figure 4b). This trend can be further observed from the PM_1 distribution (Figure 6c); hence, the average PM_1 concentration in spring was lowest at Yulin, Xian, Zhengzhou, Gucheng and Benxi. The seasonal variation patterns were very similar for PM_{10}, $PM_{2.5}$ and PM_1 at the sites in southern China.

A spatial distribution map of the seasonal average $PM_{2.5}/PM_{10}$ ratios is given in Figure 6d. For the reasons given above, lower $PM_{2.5}/PM_{10}$ ratios were observed in spring at the northern China sites, while the seasonal variation was not significant at the southern China sites.

3.4 Interannual variation

The interannual variation of $PM_{2.5}$ at various stations is presented in Figure 5. Significant decreasing trends were observed at the HBP stations of Zhengzhou and Gucheng (Figure 5a). The annual averaged $PM_{2.5}$ concentration decreased from 123.4 to 65.2 μg m^{-3} at Zhengzhou, and from 101.0 to 69.1 μg m^{-3} at Gucheng, during 2006–2014. At Zhengzhou, the lowest value of 63.7 μg m^{-3} occurred in 2012, and this level was maintained in subsequent years; however, at Gucheng, the value increased suddenly in 2012 to 95.1 μg m^{-3} and then declined rapidly during 2013 and 2014. At Xian, the annual averaged $PM_{2.5}$ concentration decreased from 2006 to 2009, increased until 2011, and then decreased again until 2014 (Figure 5a).

For the stations in northeast China, a significant increasing trend of the $PM_{2.5}$ concentration was observed at Shenyang and Benxi from 2006 to 2013, followed by a decrease in 2014 (Figure 5b). The peak value at Shenyang was especially high in 2013 at 123.1 μg m^{-3}, while the values were less than 60 μg m^{-3} in the other years. The highest values were observed in 2009 at Anshan and Dandong, but the lowest values were in 2014 at Anshan and 2010 at Dandong. A general decreasing trend was observed at Siping, with a few fluctuations. At Fushun, the value decreased from 2006 to 2011 and then increased to 2013, followed by a slight decrease in 2014.

For the stations along the middle and lower reaches of the Yangtze River, a common trend was a clearly lower $PM_{2.5}$ value in 2014 than in 2013, but the general variation trend was not significant (Figure 5c). A peak value of 33.7 μg m^{-3} was observed in 2012 at Dongtan, followed by a decrease to 24.12 μg m^{-3} over the subsequent two years. At Jinsha and Changde, the highest value was in 2013, while it was in 2009 at Lushan.

For the stations in southern China, a general decreasing trend was observed, with obvious fluctuations (Figure 5d). Panyu is a typical station in the centre of the Pearl River Delta economic area of China. The $PM_{2.5}$ value decreased from 64.6 μg m^{-3} in 2006 to 41.6 μg m^{-3} in 2014, and the lowest value was 36.4 μg m^{-3} in 2010. A similar trend was observed in Gulin, with a stronger fluctuation from 2010 to 2012. At

Nanning, a peak value occurred in 2010 and the lowest value of 28.5 μg m^{-3} was observed in 2012.

Generally, the PM_{10} and PM_1 interannual variation trends were similar to that of $PM_{2.5}$ at most stations. For example, a similar trend and fluctuations were observed at the stations presented in Figure 8 and Figure 7a. A difference in the trend was observed at Zhengzhou from 2013 to 2014, with a significant increasing trend of PM_{10} and decreasing trend of PM_1.

3.5 Diurnal variation

The average diurnal variation of $PM_{2.5}$ at various stations is presented in Figure 7. Pronounced diurnal variation of $PM_{2.5}$ was observed at most urban sites, with an obvious morning peak at around 7:00 to 8:00 a.m. and an afternoon valley between 2:00 and 4:00 p.m. At some stations, an evening peak could be recognized at around 7:00 to 9:00 p.m. (Siping, Benxi, Fushun, Anshan, Guilin and Panyu) or midnight (Gucheng, Xian). This bimodal pattern was also observed in Beijing city (Zhao et al., 2009). A unimodal pattern, without an evening peak, could be identified at some other stations (Zhengzhou, Shengyang and Nanning). In urban areas, the morning and evening peaks are contributed to by enhanced anthropogenic activity during rush hour, and the afternoon valley is mainly due to a higher atmospheric mixing layer, which is beneficial for air pollution diffusion. Panyu station is on top of a 140 m hill at the edge of Guangzhou city, so aged and mixing aerosols were observed with a weak urban diurnal variation pattern. Similar to Panyu station, the rural stations along the middle and lower reaches of the Yangtze River showed no typical urban diurnal variation pattern (Figure 7c). The diurnal variation in PM_1 and PM_{10} concentrations was similar to that of $PM_{2.5}$ at most stations.

3.6 Emission and meteorological influences

PM loadings are controlled by both emissions and meteorological conditions. Even mineral dust emissions from deserts and volatile organic compound (VOC) emissions from vegetation are controlled by meteorological factors, e.g., wind speed and temperature. The major source of air pollution in China is anthropogenic emissions, especially with the rapid economic development that has taken place in recent years. As such, the average PM concentration pattern is determined largely by emissions, but meteorological factors also play an important role by affecting pollutant diffusion and deposition.

The distributions of the anthropogenic emissions of black carbon (BC), $PM_{2.5}$, SO_2 and NO_2 in 2010, based on the HTAP_v2 harmonized emissions database (http://iek8wikis.iek.fz-juelich.de/HTAPWiki/WP1.1), are presented in Figure 8. The emissions data for the East Asia domain were supplied by the MICS-Asia project. The spatial distributions of species show a consistent pattern with the high emissions regions of the HBP, Guanzhong Plain, Sichuan Basin, middle and lower reaches of the Yangtze River, Pearl River Delta region, and the industrial region of northeast China, which is generally similar to the PM loadings pattern for China (Figure 1). For example, most stations subjected to PM pollution are located in the highest emissions region of the HBP. This indicates that average PM loadings are controlled by the quantity of anthropogenic emissions in central-eastern China.

The trends in emissions for China during 2005–2010 (Wang et al., 2014b) show that emissions of SO_2 and $PM_{2.5}$ in East Asia decreased by 15% and 12 %, respectively, while emissions of NOx and non-methane VOCs increased by 25% and 15%, respectively. Driven by changes in emissions, $PM_{2.5}$ concentrations decreased by 2–17 μg m^{-3} over most of the North China Plain, the Yangtze River Delta and the Pearl River Delta (Zhao et al., 2013). This could explain the general decreasing trend with respect to PM during 2006–2010 at most stations (Figure 5). The spatial distributions of emissions differences between 2010 and 2008 for BC, $PM_{2.5}$, SO_2 and NO_2 are plotted in Figure 9, based on the HTAP_v2 emission dataset. BC emissions decreased from 2008 to 2010 in most regions of east China, except the provinces of Hebei, Shanxi, Hubei, Jiangxi and Inner Mongolia (Figure 9a). More areas of China showed a reduction in $PM_{2.5}$ emissions, except Shanxi and Hubei provinces (Figure 9b). The SO_2 emissions difference (Figure 9c) showed a similar pattern to that of BC but with an increasing trend apparent in northeast China. NOx emissions increased in most regions of central-eastern China, except in the provinces of Guangdong, Zhejiang and Taiwan (Figure 9d). This trend was driven by the rapid growth of industry and transportation, combined with inadequate control strategies (Wang et al., 2014b).

Although there are no published emissions data after 2010, it is believed that emissions have to a certain extent been controlled well since the end of 2013, with the arrival of China's "Action Plan for the Control of Air Pollution" document. This could explain the general decreasing trend for the year 2014 at most stations (Figure

5).

Central-eastern China experienced severe haze events in January 2013, with a regionally stable planetary boundary layer and low mixing height (Wang et al., 2014a). The daily averaged $PM_{2.5}$ concentrations and meteorological factors of wind speed and relative humidity for this period at Zhengzhou, Shenyang and Nanning are plotted in Figure 10. Zhengzhou is located in this haze region, and experienced very high $PM_{2.5}$ concentrations, especially from Jan. 6 to 15. The wind speed variation was negatively related with $PM_{2.5}$ concentrations. The rapid increase in $PM_{2.5}$ concentrations from Jan. 1 to 6 corresponded with the rapid decrease in wind speed during the same period. Also, the strong wind speed on Jan. 24 resulted in the low $PM_{2.5}$ concentration. Shenyang and Nanning are not located in this severe haze region, but still suffered some fine PM days that month. A negative correlation between $PM_{2.5}$ and wind speed was also observed at Shengyang and Nanning. In general, relative humidity (RH) was positively related with the $PM_{2.5}$ concentration if no precipitation occurred. Otherwise, high RH with precipitation corresponded to low PM concentrations due to wet deposition.

In terms of interannual variation, the negative correlation between $PM_{2.5}$ concentrations and wind speed, and the positive correlation between $PM_{2.5}$ concentrations and relative humidity, could not be well identified (Figure 11). Although a generally similar variation trend for the PM_{10} concentration and relative humidity was observed at Zhengzhou, this was not found at other stations. The $PM_{2.5}$ concentration in 2014 was lower than in 2013, but the relative humidity was much higher and the wind speed much lower. The interannual variation of PM concentrations could not be explained solely by meteorological factors, although a recent model simulation for the period 2004–2012 with anthropogenic emissions fixed at the values for the year 2006 indicated that variations in meteorological fields dominated the interannual variation in aerosols in China (Mu and Liao, 2014). Long-term, both emissions and meteorological factors play important roles; while in the short-term, meteorological factors play a leading role—at least in the absence of significant emissions changes.

4 Conclusion

Spatial and temporal trends in PM pollution were examined using PM_{10}, $PM_{2.5}$ and PM_1 concentration data at 24 stations from 2006 to 2014. Relatively high PM concentrations were observed at most stations. There were 14 stations that reached the PM_{10} annual air quality standard, but only 7 stations, mostly rural and remote stations, reached the $PM_{2.5}$ annual air quality standard of China. The highest PM concentrations were observed at the stations on the HBP and Guanzhong Plain. In addition, the percentage value of substandard days of $PM_{2.5}$ was greater than 50%, indicating very serious air pollution in these regions. PM pollutants are also a serious problem in the industrial regions of northeast China and the Sichuan basin. The PM concentrations were relatively lower in southern areas of China, but the averaged $PM_{2.5}$ concentration was still higher than the national standard.

Given they are both fine particles, PM_1 and $PM_{2.5}$ were more closely correlated than $PM_{2.5}$ and PM_{10}. The correlations were sensitive to the effect of outlier data at those stations heavily impacted by dust storm events. More dust aerosol was observed in northern China, and thus the $PM_{2.5}/PM_{10}$ ratios increased from less than 0.6 to around 0.9 when moving from north to south China.

Pronounced seasonal variations were observed at most stations, with the highest concentrations in winter and lowest concentrations in summer. PM_{10} concentrations were also high in spring, due to the contribution of dust storm events, especially at those stations near to dust source regions. For $PM_{2.5}$ and PM_1, spring was a relatively low concentration season, especially at the stations in northern China. Also, low $PM_{2.5}/PM_{10}$ ratios were observed in spring in northern China.

An interannual decreasing trend was observed in the HBP and southern China from 2006 to 2014, but an increasing trend occurred at some stations in northeast China, and no significant trend could be found over the middle and lower reaches of the Yangtze River. Annual-averaged PM concentrations were lower in 2014 than 2013 at most stations, which may indicate an improvement in air quality following the "Action Plan for the Control of Air Pollution" document issued by the Chinese government in September 2013.

Bimodal and unimodal diurnal variation patterns were identified at urban stations. A negative correlation between PM concentrations and wind speed was found in for the short-term, but variations in emissions must be considered for long-term trend analyses, especially in rapidly developing countries.

This network-based observation dataset provides the longest continuous record of fine particle concentrations in China, but it features a limited number of stations and an uneven spatial distribution. Importantly, there is no representative city site in the Yangtze River delta region, which is an important haze area in China. The emissions sources and meteorological factors influencing PM spatial and temporal patterns in China still require further study.

Acknowledgements

This work was supported by grants from the National Key Project of Basic Research (2014CB441201), the National Natural Science Foundation of China (41275167) and the Chinese Academy of Meteorological Sciences (2013Z007). It was also supported by the Climate Change Collaborative Innovation Center and the CMA Innovation Team of Haze-fog Observation and Forecasts.

References:

Brook, J. R., Dann, T. F., and Burnett, R. T.: The relationship among TSP, PM10, PM2.5, and Inorganic constituents of atmospheric particulate matter at multiple Canadian locations. J. Air Waste Manage. Assoc. 47, 2-19, 1997.

Cao, J.-J., Shen, Z.-X., Chow, J. C., Watson, J. G., Lee, S.-C., Tie, X.-X., Ho, K.-F., Wang, G.-H., and Han, Y.-M.: Winter and Summer PM2.5 Chemical Compositions in Fourteen Chinese Cities. J. Air Waste Manage. Assoc. 62, 1214-1226, 2012.

Chen, S., Huang, J., Zhao, C., Qian, Y., Leung, R., and Yang, B.: Modeling the transport and radiative forcing of Taklimakan dust over the Tibetan Plateau: A case study in the summer of 2006. J. Geophys. Res. 118, 797-812, 2013.

Delfino, R. J., Sioutas, C., and Malik, S.: Potential role of ultrafine particles in associations between airborne particle mass and cardiovascular health. Environ. Health Persp. 113, 934-946, 2005.

Eeftens, M., Tsai, M.-Y., Ampe, C., Anwander, B., Beelen, R., Bellander, T., Cesaroni, G., Cirach, M., Cyrys, J., Hoogh, K. d., Nazelle, A. D., Vocht, F. d., Declercq, C., Dedele, A., Eriksen, K., Galassi, C., Grazuleviciene, R., Grivas, G., Heinrich, J., Hoffmann, B., Iakovides, M., Ineichen, A., Katsouyanni, K., Korek, M., Krämer, U., Kuhlbusch, T., Lanki, T., Madsen, C., Meliefste, K., Mölter, A., Moslerm, G., Nieuwenhuijsen, M., Oldenwening, M., Pennanen, A., Probst-Hensch, N., Quass, U., Raaschou-Nielsen, O., Ranzi, A., Stephanou, E., Sugiri, D., Udvardy, O., Vaskövi, É., Weinmayr, G., Brunekreef, B., and Hoek, G.: Spatial variation of $PM_{2.5}$, PM_{10}, $PM_{2.5}$ absorbance and PMcoarse concentrations between and within 20 European study areas and the relationship with NO_2 - Results of the ESCAPE project. Atmos. Environ. 62, 303-317, 2012.

Eldred, R. A., Cahill, T. A., and Flocchini, R. G.: Composition of PM2.5 and PM10 aerosols in the IMPROVE network. J. Air Waste Manage. Assoc. 47, 194-203, 1997.

Gehrig, R., and Buchmann, B.: Characterising seasonal variations and spatial distribution of ambient PM10 and PM2.5 concentrations based on long-term Swiss monitoring data. Atmos. Environ. 37, 2571-2580, 2003.

Gomiscek, B., Hauck, H., Stopper, S., and Preining, O.: Spatial and temporal variations of PM_1, $PM_{2.5}$, PM_{10} and particle number concentration during the AUPHEP - project. Atmos. Environ. 38, 3917-3934, 2004.

Grimm, H., and Eatough, D. J.: Aerosol Measurement: The Use of Optical Light Scattering for the Determination of Particulate Size Distribution, and Particulate Mass, Including the Semi-Volatile Fraction. J. Air Waste Manage. Assoc. 59, 101-107, 2009.

Hansen, J. C., Woolwine, W. R., Bates, B. L., Clark, J. M., Kuprov, R. Y., Mukherjee, P., Murray, J. A., Simmons, M. A., Waite, M. F., Eatough, N. L., Eatough, D. J., Long, R., and Grover, B. D.: Semicontinuous $PM_{2.5}$ and PM_{10} mass and composition measurements in Lindon, Utah, during winter 2007. J. Air & Waste Manage. Assoc. 60, 346-355, 2010.

Haywood, J., and Boucher, O.: Estimates of the direct and indirect radiative forcing due to tropospheric aerosols: A review. Rev. Geophys. 38, 513-543, 2000.

He, K., Yang, F., Ma, Y., Zhang, Q., Yao, X., Chan, C. K., Cadle, S., Chan, T., and Mulawa, P.: The characteristics of PM2.5 in Beijing, China. Atmos. Environ. 35, 4959-4970, 2001.

Houthuijs, D., Breugelmans, O., Hoek, G., Vaskövi, É., Mihάliková, E., Pastuszka, J. S., Jirik, V., Sachelarescu, S., Lolova, D., Meliefste, K., Uzunova, E., Marinescu, C., Volf, J., Leeuw, F. d., Wiel, H. v. d., Fletcher, T., Lebret, E., and Brunekreef, B.: PM10 and PM2.5 concentrations in Central and Eastern Europe: results from the Cesar study. Atmos. Environ. 35, 2757-2771, 2001.

Janssen, N. A. H., Fischer, P., Marra, M., Ameling, C., and Cassee, F. R.: Short-term effects of $PM_{2.5}$, PM_{10} and $PM_{2.5-10}$ on daily mortality in the Netherlands. Sci. Total Environ. 463-464, 20-26, 2013.

Li, C., Mao, J., Lau, K.-H. A., Chen, J.-C., Yuan, Z., Liu, X., Zhu, A., and Liu, G.: Characteristics of distribution and seasonal variation of aerosol optical depth in eastern China with MODIS products. Chinese Sci. Bull. 48, 2488-2495, 2003.

Luo, Y., Lu, D., Zhou, X., Li, W., and He, Q.: Characteristics of the spatial distribution and yearly variation of aerosol optical depth over China in last 30 years. J. Geophys. Res. 106, 14501-14513, 2001.

Malm, W. C., Schichtel, B. A., Pitchford, M. L., Ashbaugh, L. L., and Eldred, R. A.: Spatial and monthly trends in speciated fine particle concentration in the United States. J. Geophys. Res. 109, D03306, doi:10.1029/2003JD003739, 2004.

Mu, Q., and Liao, H.: Simulation of the interannual variations of aerosols in China: role of variations in meteorological parameters. Atmos. Chem. Phys. 14, 9597-9612, 2014.

Oberdörster, G., Oberdörster, E., and Oberdörster, J.: Nanotoxicology: An Emerging Discipline Evolving from Studies of Ultrafine Particles. Environ. Health Persp. 113, 823-839, 2005.

Pope III, C. A., and Dockery, D. W.: Health effects of fine particulate air pollution: Lines that connect. J. Air Waste Manage. Assoc. 56, 709-742, 2006.

Qian, W. H., Tang, X., and Quan, L. S.: Regional characteristics of dust storms in China. Atmos. Environ. 38, 4895-4907, 2004.

Qu, W.-J., Zhang, X.-Y., Arimoto, R., Wang, Y.-Q., Wang, D., Sheng, L.-F., and Fu, G.: Aerosol background at two remote CAWNET sites in western China. Sci. Total Environ. 407, 3518-3529, 2009.

Qu, W. J., Arimoto, R., Zhang, X. Y., Zhao, C. H., Wang, Y. Q., Sheng, L. F., and Fu, G.: Spatial distribution and interannual variation of surface PM_{10} concentrations over eighty-six Chinese cities. Atmos. Chem. Phys. 10, 5641-5662, 2010.

Ramanathan, V., Crutzen, P. J., Kiehl, J. T., and Rosenfeld, D.: Aerosols, climate, and the hydrological cycle. Science 294, 2119-2124, 2001.

Sciare, J., Cachier, H., Sarda-Este`ve, R., Yu, T., and Wang, X.: Semi-volatile aerosols in Beijing (R.P. China): Characterization and influence on various PM2.5 measurements. J. Geophys. Res. 112, D18202, doi:10.1029/2006JD007448, 2007.

Tiwari, S., Chate, D. M., Pragya, P., Ali, K., and Bisht, D. S.: Variations in Mass of the PM10, PM2.5 and PM1 during the Monsoon and Winter at New Delhi. Aerosol and Air Quality Research 12, 20-29, 2012.

Wang, G., Huang, L., Gao, S., Gao, S., and Wang, L.: Measurements of PM_{10} and $PM_{2.5}$ in urban area of Nanjing, China and the assessment of pulmonary deposition of particle mass. Atmos. Environ. 48, 689-695, 2002.

Wang, H., Xu, J., Zhang, M., Yang, Y., Shen, X., Wang, Y., Chen, D., and Guo, J.: A study of the meteorological causes of a prolonged and severe haze episode in January 2013 over central-eastern China. Atmospheric Environment 98, 146-157, 2014a.

Wang, S. X., Zhao, B., Cai, S. Y., Klimont, Z., Nielsen, C. P., Morikawa, T., Woo, J. H., Kim, Y., Fu, X., Xu, J. Y., Hao, J. M., and He, K. B.: Emission trends and mitigation options for air pollutants in East Asia. Atmos. Chem. Phys. 14, 6571-6603, 2014b.

Wang, X., Bi, X., Sheng, G., and Fu, J.: Chemical composition and sources of PM10 and PM2.5 aerosols in Guangzhou, China. Environ. Monit. Assess. 119, 425-439, 2006.

Wang, Y. Q., Zhang, X. Y., Gong, S. L., Zhou, C. H., Liu, H. L., Niu, T., and Yang, Y. Q.: Surface observation of sand and dust storm in East Asia and its application in CUACE/Dust. Atmos. Chem. Phys. 8, 545-553, 2008.

Watson, J.: Visibility: Science and Regulation. J. Air Waste Manage. Assoc. 52, 628-713, 2002.

Wei, F., Teng, E., Wu, G., Hu, W., Wilson, W. E., Chapman, R. S., Pau, J. C., and Zhang, J.: Ambient concentrations and elemental composition of PM_{10} and $PM_{2.5}$ in four Chinese cities. Environ. Sci. Technol. 33, 4188-4193, 1999.

Yao, X., Chan, C. K., Fang, M., Cadle, S., Chan, T., Mulawa, P., He, K., and Ye, B.: The water-soluble ionic composition of PM2.5 in Shanghai and Beijing, China. Atmos. Environ. 36, 4223-4234, 2002.

Zhang, Q., Streets, D. G., Carmichael, G. R., He, K. B., Huo, H., Kannari, A., Klimont, Z., Park, I. S., Reddy, S., Fu, J. S., Chen, D., Duan, L., Lei, Y., Wang, L. T., and Yao, Z. L.: Asian emissions in 2006 for the NASA INTEX-B mission. Atmos. Chem. Phys. 9, 5131-5153, 2009.

Zhang, X. Y., Gong, S. L., Zhao, T. L., Arimoto, R., Wang, Y. Q., and Zhou, Z. J.: Sources of Asian dust and role of climate change versus desertification in Asian dust emission. Geophys. Res. Lett. 30, 2272 10.1029/2003GL018206, 2003.

Zhang, X. Y., Wang, Y. Q., Niu, T., Zhang, X. C., Gong, S. L., Zhang, Y. M., and Sun, J. Y.: Atmoshperic aerosol compositions in China: spatial/temporal variability, chemical signature, regional haze distribution and comparisons with global aerosols. Atmos. Chem. Phys. 12, 779-799, 2012.

Zhao, B., Wang, S., Dong, X., Wang, J., Duan, L., Fu, X., Hao, J., and Fu, J.: Environmental effects of the recent emission changes in China: implications for particulate matter pollution and soil acidification. Environ. Res. Lett. 8, 024031, doi:10.1088/1748-9326/8/2/024031, 2013.

Zhao, X., Zhang, X., Pu, W., Meng, W., and Xu, X.: Scattering properties of the atmospheric aerosol in Beijing, China. Atmos. Res. 101, 799-808, 2011.

Zhao, X., Zhang, X., Xu, X., Xu, J., Meng, W., and Pu, W.: Seasonal and diurnal variations of ambient PM2.5 concentration in urban and rural environments in Beijing. Atmos. Environ. 43, 2893-2900, 2009.

Zheng, M., Salmon, L. G., Schauer, J. J., Zeng, L., Kiang, C. S., Zhang, Y., and Cass, G. R.: Seasonal trends in PM2.5 source contributions in Beijing, China. Atmos. Environ. 39, 3967-3976, 2005.

Zhou, Z. J., and Zhang, G. C.: Typical severe dust storms in northern China during 1954-2002. Chinese Sci. Bull. 48, 2366-2370, 2003.

Table 1. Description of the PM stations.

Stations	Latitude (ºN)	Longitude (º E)	Altitude (m)	Start Time	Description
Zhengzhou	34.78	113.68	99.0	1/2006	Urban, in the center of Zhengzhou city, 56 m building.
Chengdu	30.65	104.04	496.0	3/2006	Urban, in the center of Chengdu city, 91 m building.
Xian	34.43	108.97	363.0	1/2006	Urban, in northern margin of Xian city, 20 km north of center of Xian city, 4 m sampling container.
Nanning	22.82	108.35	84.0	1/2006	Urban, in Nanning city, 140 m hill.
Anshan	41.05	123.00	78.3	10/2007	Urban, in Anshan city, 10 m building.
Shenyang	41.76	123.41	110.0	10/2007	Urban, in Shenyang city, 15m building.
Benxi	41.19	123.47	185.4	10/2007	Urban, in Benxi city, 12 m building.
Fushun	41.88	123.95	163.0	10/2007	Urban, in Fushun city, 10 m building.
Qingdao	36.07	120.33	77.2	3/2007	Urban, in Qingdao city, top of Fulongshan hill.
Lhasa	29.67	91.13	3663.0	1/2006	Urban, in Lhasa city, 7 m building.
Siping	43.18	124.33	165.4	3/2007	Urban, in Siping city, 4 m sampling container.
Panyu	23.00	113.35	5.0	1/2006	Suburban, in Panyu district of Guangzhou city, 140 m hill.
Gucheng	39.13	115.80	15.2	1/2006	Suburban, 38 km southwest of Baoding city, within area of rapid urbanization, 8 m building.
Chifeng	42.27	118.97	568.0	3/2007	Rural, suburbs of Chifeng city, 4 m sampling container.
Dandong	40.05	124.33	13.9	3/2007	Rural, suburbs of Dandong city, 4 m sampling container.
Erlianhaote	43.65	111.97	965.9	3/2007	Rural, suburbs of Erlianhaote city, 4 m sampling container.
Yulin	38.43	109.20	1135.0	1/2006	Rural, 10 km north of Yulin city, at the southeastern edge of Mu Us desert.
Jinsha	29.63	114.20	416.0	4/2006	Rural, 105 km north of Wuhan city, 8 m building.
Guilin	25.32	110.30	164.4	1/2006	Rural, north margin of Guilin

					city, meteorological observation field.
Lushan	29.57	115.99	1165.0	1/2006	Rural, Kuniubei peak of Mount Lu.
Changde	29.17	111.71	563.0	1/2006	Rural, 18 km northwest from Changde city, 8 m building.
Dongtan	31.50	121.80	10.0	5/2009	Rural, east of Chongming island near Shanghai.
Akdala	47.12	87.97	562.0	9/2006	Remote, 55 km west of Fuhai county, 10 m building.
Shangri-La	28.02	99.73	3580.0	10/2006	Remote, 12 km northeast of Shangri-La county.

Table 2. Averaged PM_{10}, $PM_{2.5}$ and PM_1 concentrations and their interrelationships at each station.

Stations	Averaged PM concentrations ($\mu g\ m^{-3}$)[a]			SB ratio (PM_{10})[b]	SB ratio ($PM_{2.5}$)[b]	$PM_{2.5}$/PM_{10}	PM_1/$PM_{2.5}$	R^2 ($PM_{2.5}$ to PM_{10})	R^2 (PM_1 to $PM_{2.5}$)
	PM_{10}	$PM_{2.5}$	PM_1						
Zhengzhou	131.7 (84.4)	84.8 (47.4)	71.0 (40.5)	0.31	0.51	0.68	0.84	0.68	0.91
Chengdu	78.0 (72.5)	59.5 (42.2)	52.7 (35.4)	0.11	0.27	0.83	0.91	0.76	0.94
Xian	135.4 (97.3)	93.6 (67.3)	77.0 (55.6)	0.34	0.52	0.73	0.83	0.77	0.93
Nanning	51.2 (56.3)	38.4 (24.7)	34.9 (22.2)	0.01	0.08	0.77	0.91	0.52	0.97
Anshan	97.8 (62.9)	60.9 (42.9)	52.3 (39.0)	0.17	0.25	0.65	0.85	0.72	0.98
Shenyang	85.0 (58.2)	59.1 (42.7)	50.8 (36.7)	0.11	0.25	0.69	0.85	0.88	0.97
Benxi	97.6 (57.4)	66.7 (45.0)	54.8 (36.4)	0.13	0.30	0.69	0.82	0.81	0.94
Fushun	80.3 (54.2)	50.1 (31.7)	42.8 (28.3)	0.07	0.17	0.66	0.85	0.64	0.97
Qingdao	64.8 (52.1)	47.3 (34.0)	41.1 (30.5)	0.05	0.17	0.76	0.86	0.76	0.95
Lhasa	37.7 (30.8)	14.0 (10.7)	9.6 (8.6)	0.01	0.00	0.40	0.66	0.72	0.94
Panyu	58.7 (33.1)	44.5 (24.4)	39.7 (22.1)	0.02	0.12	0.77	0.89	0.95	0.98
Gucheng	127.8 (75.1)	89.7 (53.0)	79.4 (48.8)	0.31	0.54	0.71	0.87	0.79	0.97
Siping	83.3 (54.3)	55.4 (35.2)	48.5 (32.5)	0.10	0.22	0.68	0.86	0.71	0.96
Chifeng	88.0 (68.9)	42.4 (33.1)	32.6 (27.8)	0.17	0.14	0.51	0.75	0.72	0.92
Dandong	66.8 (44.0)	45.6 (24.8)	39.3 (21.3)	0.03	0.11	0.71	0.86	0.64	0.90
Erlianhaote	49.1 (80.2)	22.0 (22.6)	15.9 (14.7)	0.03	0.03	0.51	0.72	0.71	0.61
Yulin	66.6 (67.1)	31.2 (21.0)	22.4 (15.9)	0.06	0.03	0.54	0.72	0.54	0.61
Jinsha	42.0 (38.6)	33.6 (24.1)	30.5 (21.9)	0.01	0.06	0.85	0.90	0.63	0.89
GuiLin	57.6	46.5	41.7	0.04	0.15	0.85	0.90	0.70	0.96

	(50.5)	(30.8)	(27.1)						
Lushan	45.4 (32.7)	37.8 (27.9)	33.2 (26.7)	0.01	0.09	0.85	0.86	0.91	0.95
Changde	45.7 (33.8)	40.3 (29.1)	37.0 (27.5)	0.01	0.12	0.89	0.91	0.93	0.96
Dongtan	31.9 (34.0)	27.4 (25.9)	24.8 (23.8)	0.01	0.06	0.90	0.90	0.92	0.96
Akdala	17.1 (57.6)	9.8 (13.7)	7.7 (6.9)	0.00	0.00	0.67	0.79	0.80	0.53
Shangri-La	6.8 (6.3)	5.2 (5.3)	4.5 (5.0)	0.00	0.00	0.76	0.81	0.94	0.99

[a]Arithmetic mean value with standard deviation in parentheses.

[b]The ratio of substandard days (daily averaged PM_{10} or $PM_{2.5}$ concentrations that exceed the standard values) to total observation days.

Figure Captions

Figure 1. Map showing the PM observation stations and bar charts for their average PM_{10}, $PM_{2.5}$ and PM_1 concentrations (μg m^{-3}).

Figure 2. Scatterplots of PM_1 versus $PM_{2.5}$ (a) with and (b) without data from the strong sand and dust storm at Akdala.

Figure 3. Spatial distribution of the average ratios of (a) $PM_{2.5}/PM_{10}$ and (b) $PM_1/PM_{2.5}$.

Figure 4. Spatial distribution of the seasonal average concentrations (μg m^{-3}) of (a) PM_{10}, (b) $PM_{2.5}$, (c) PM_1 and (d) ratios of $PM_{2.5}/PM_{10}$.

Figure 5. Interannual variations of $PM_{2.5}$ concentrations at the stations (a) on the HBP and Guanzhong Plain, (b) in northeast China, (c) along the middle and lower reaches of the Yangtze River, and (d) in southern China.

Figure 6. Interannual variation of (a) PM_{10} concentration and (b) PM_1 concentration at Zhengzhou, Xian and Gucheng.

Figure 7. Diurnal variation of $PM_{2.5}$ concentrations at the stations (a) on the HBP and Guanzhong Plain, (b) in northeast China, (c) along the middle and lower reaches of the Yangtze River, and (d) in southern China.

Figure 8. Anthropogenic emission distributions at a resolution of 0.1° × 0.1°, based on HTAP_v2 dataset: (a) BC; (b) $PM_{2.5}$; (c) SO_2; (d) NOx (units: kg m^{-2} s^{-2}).

Figure 9. Emissions differences between 2010 and 2008 at a resolution of 0.1° × 0.1°, based on HTAP_v2 dataset: (a) BC; (b) $PM_{2.5}$; (c) SO_2; (d) NOx (units: kg m^{-2} s^{-2}).

Figure 10. Daily averaged $PM_{2.5}$ concentrations vs wind speed and relative humidity at Zhengzhou, Shenyang and Nanning in January 2013.

Figure 11. Interannual variation of PM_{10}, $PM_{2.5}$ and PM_1 vs wind speed and relative humidity at Zhengzhou and Nanning.

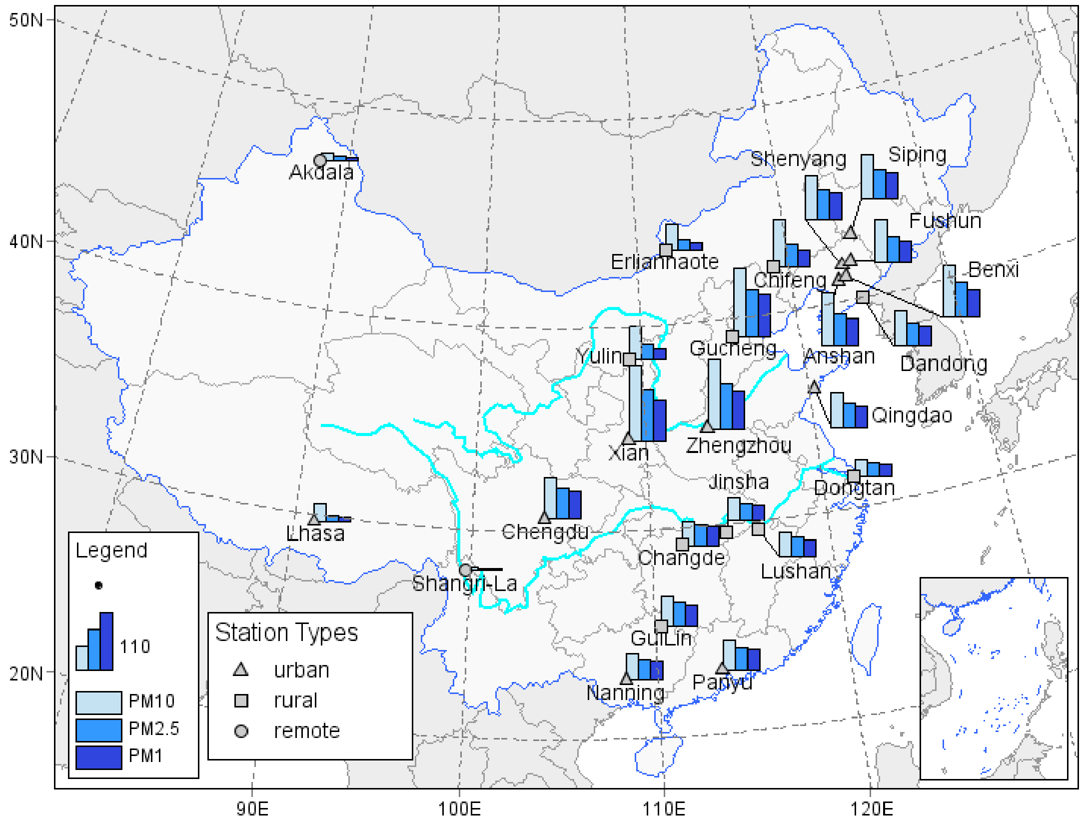

Figure 1. Map showing the PM observation stations and bar charts for their average PM_{10}, $PM_{2.5}$ and PM_1 concentrations (μg m^{-3}).

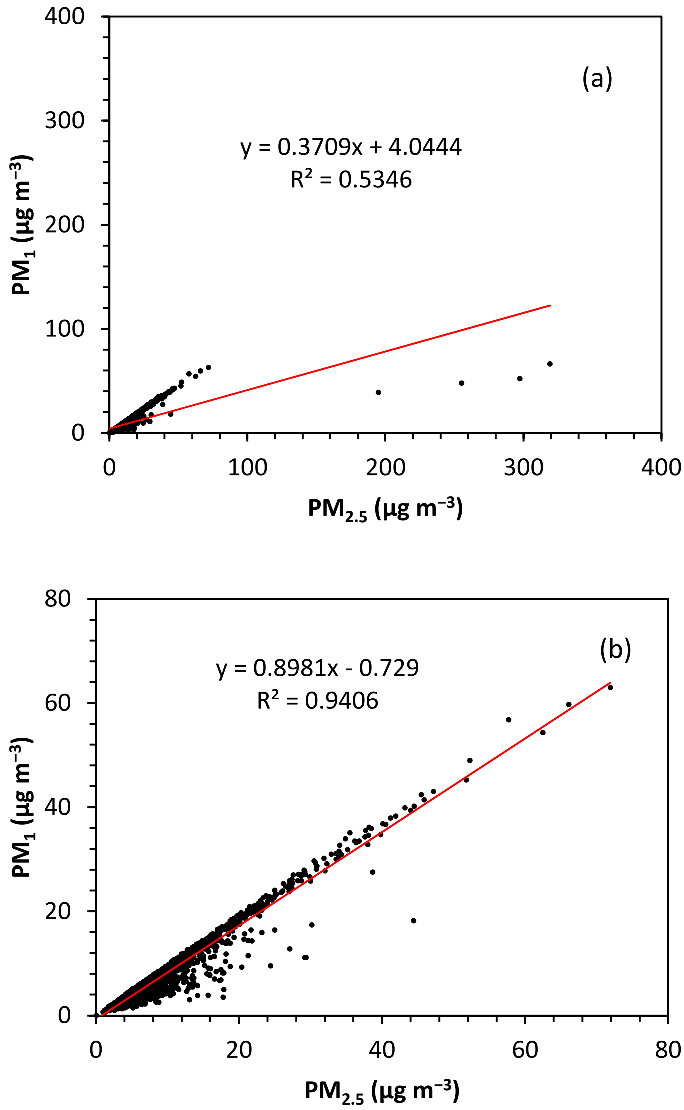

Figure 2. Scatterplots of PM_1 versus $PM_{2.5}$ (a) with and (b) without data from the strong sand and dust storm at Akdala.

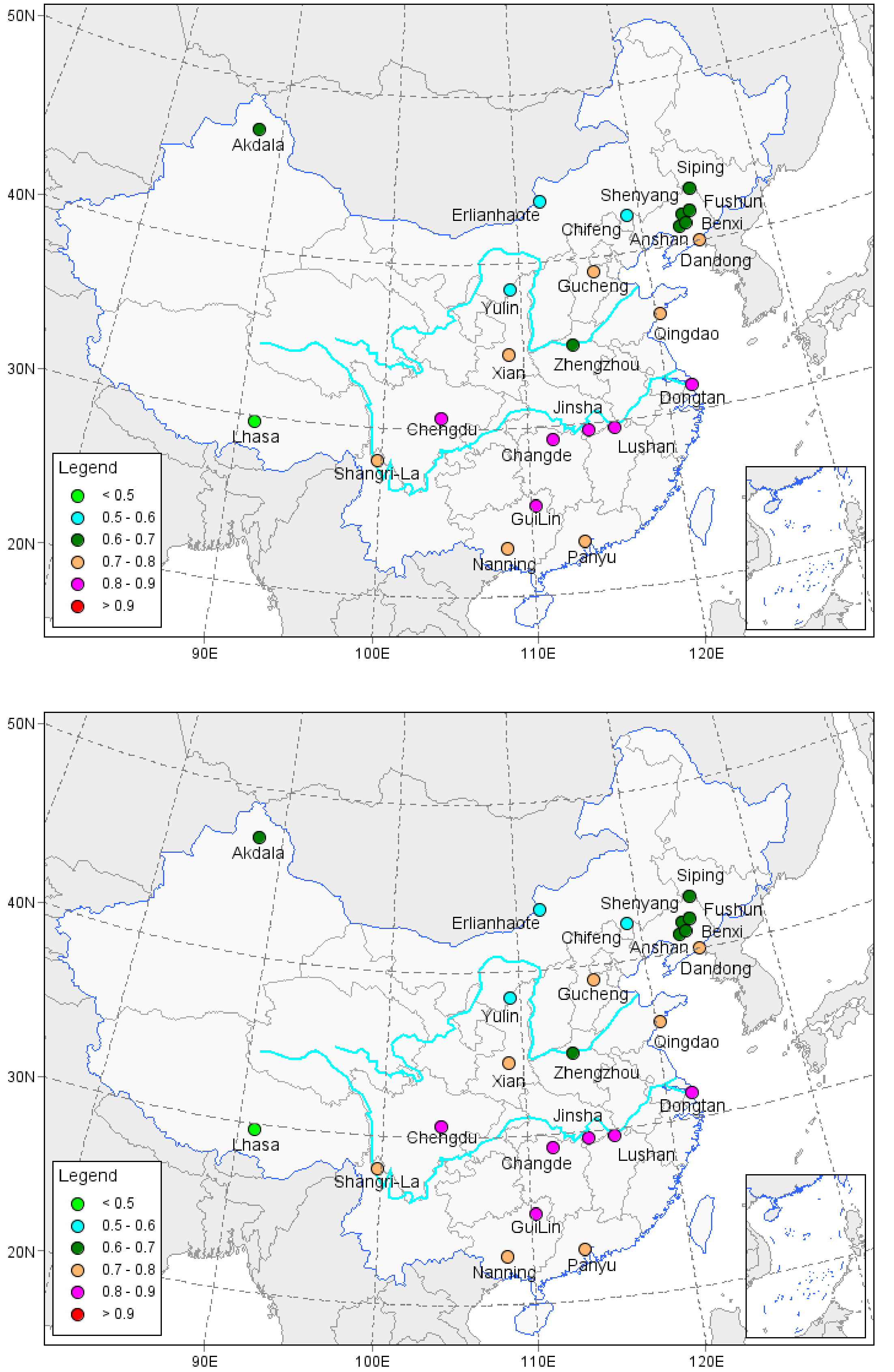

Figure 3. Spatial distribution of the average ratios of (a) $PM_{2.5}/PM_{10}$ and (b) $PM_1/PM_{2.5}$.

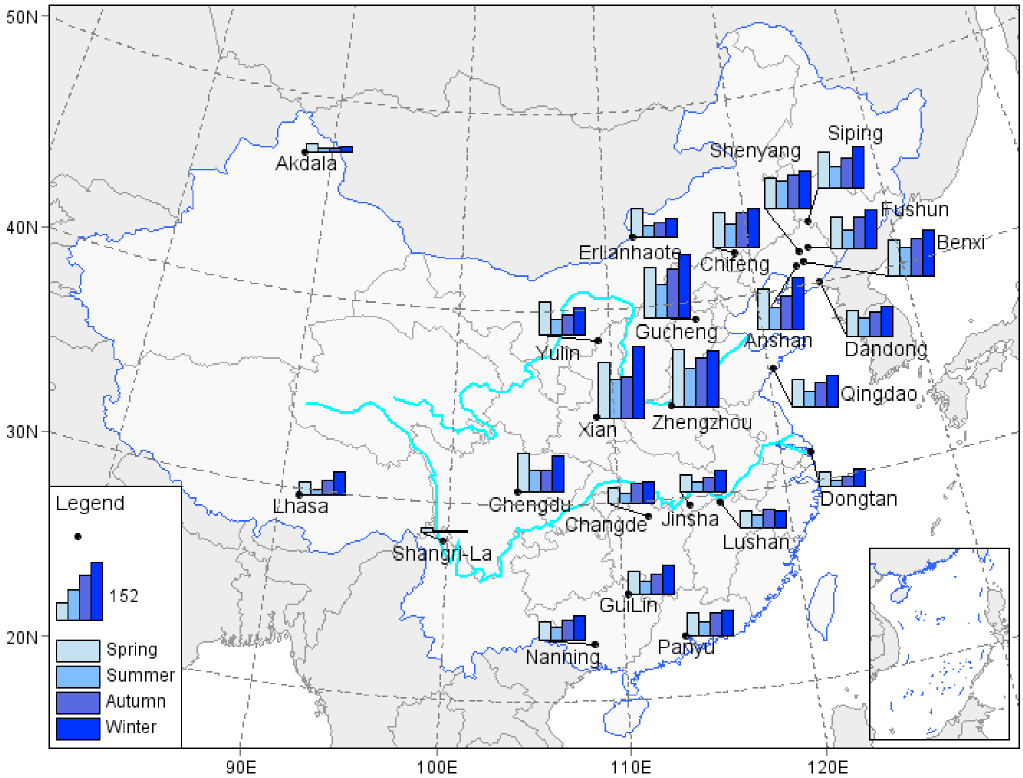
50N
40N
30N
20N
90E
100E
110E
120E
Akdala
Shenyang
Siping
Fushun
Benxi
Erlianhaote
Chifeng
Gucheng
Anshan
Dandong
Yulin
Qingdao
Xian
Zhengzhou
Lhasa
Chengdu
Changde
Jinsha
Dongtan
Lushan
Shangri-La
GuiLin
Nanning
Panyu
Legend
152
Spring
Summer
Autumn
Winter

(a)

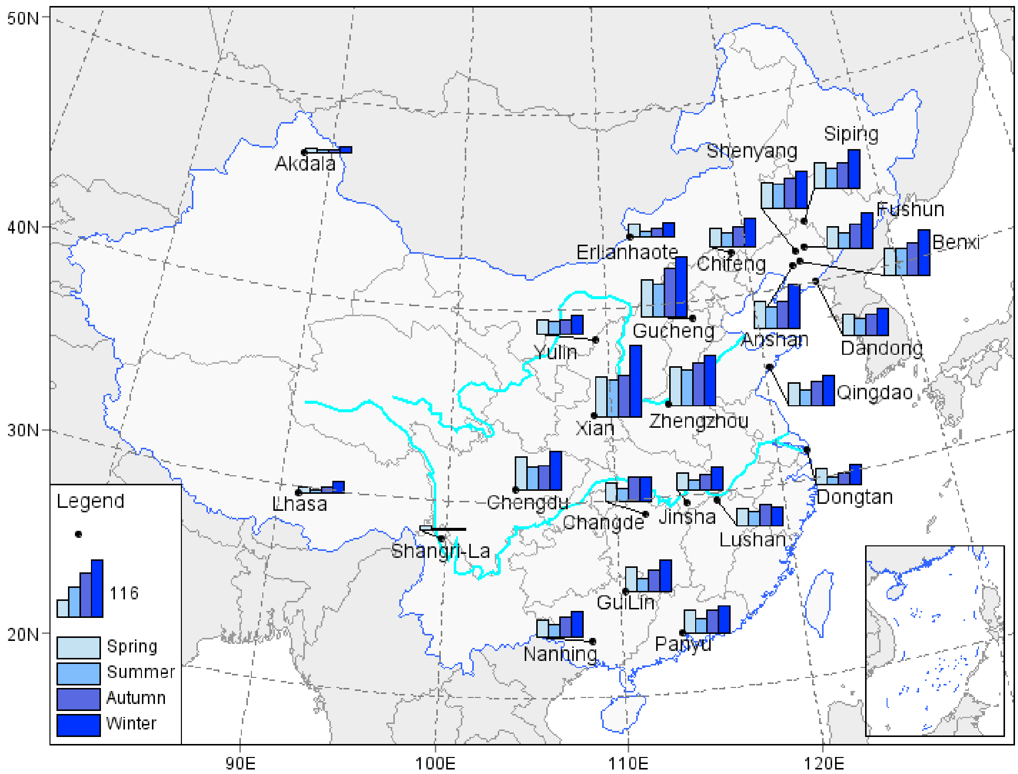
50N
40N
30N
20N
90E
100E
110E
120E
Akdala
Shenyang
Siping
Fushun
Benxi
Erlianhaote
Chifeng
Gucheng
Anshan
Dandong
Yulin
Qingdao
Xian
Zhengzhou
Lhasa
Chengdu
Changde
Jinsha
Dongtan
Lushan
Shangri-La
GuiLin
Nanning
Panyu
Legend
116
Spring
Summer
Autumn
Winter

(b)

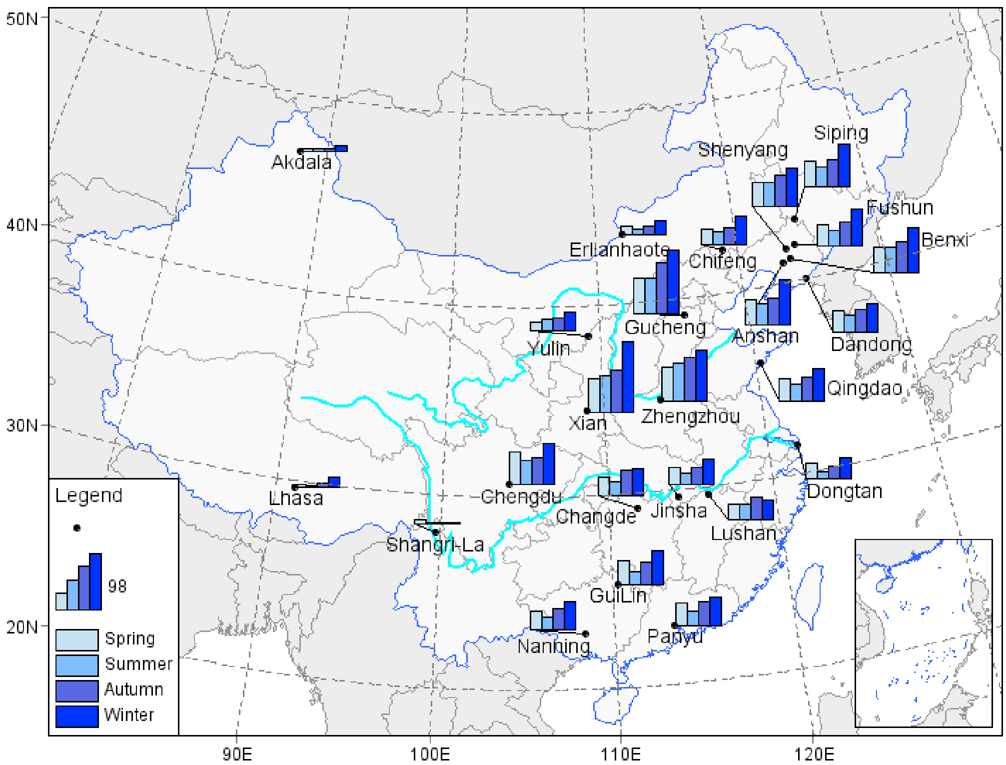

(c)

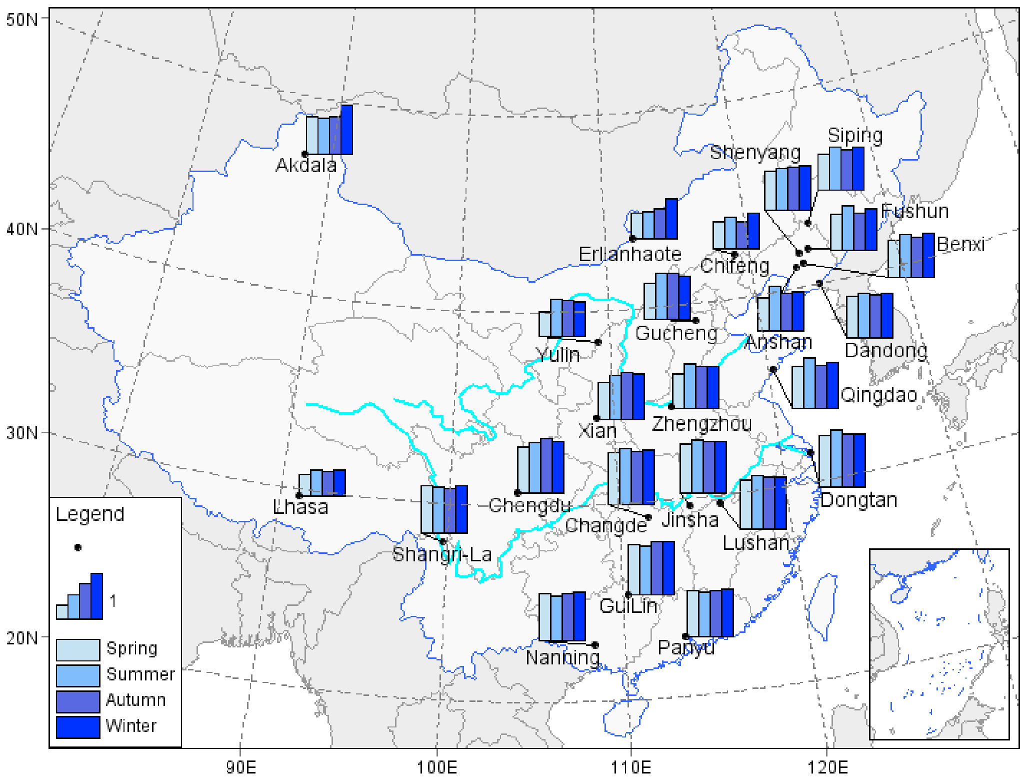

(d)

Figure 4. Spatial distribution of the seasonal average concentrations (μg m^{-3}) of (a) PM_{10}, (b) $PM_{2.5}$, (c) PM_1 and (d) ratios of $PM_{2.5}/PM_{10}$.

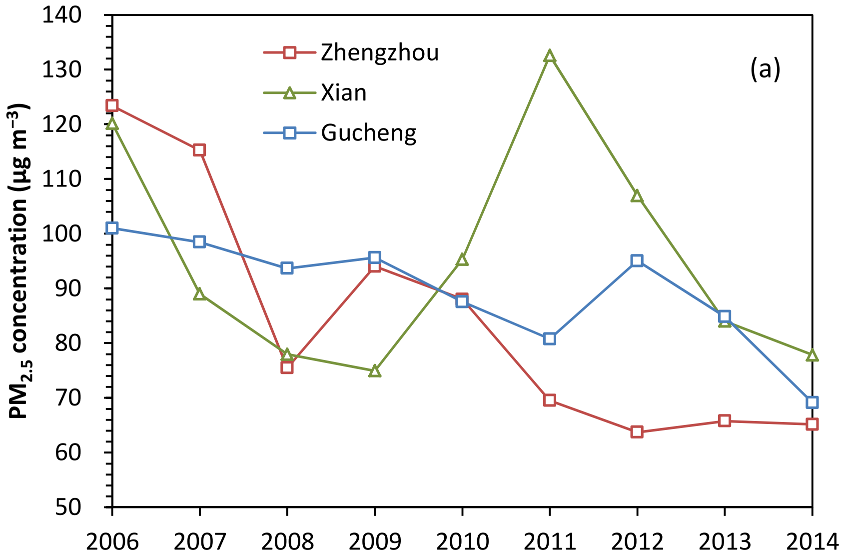

Zhengzhou
Xian
Gucheng
(a)
PM2.5 concentration (µg m−3)
140
130
120
110
100
90
80
70
60
50
2006
2007
2008
2009
2010
2011
2012
2013
2014

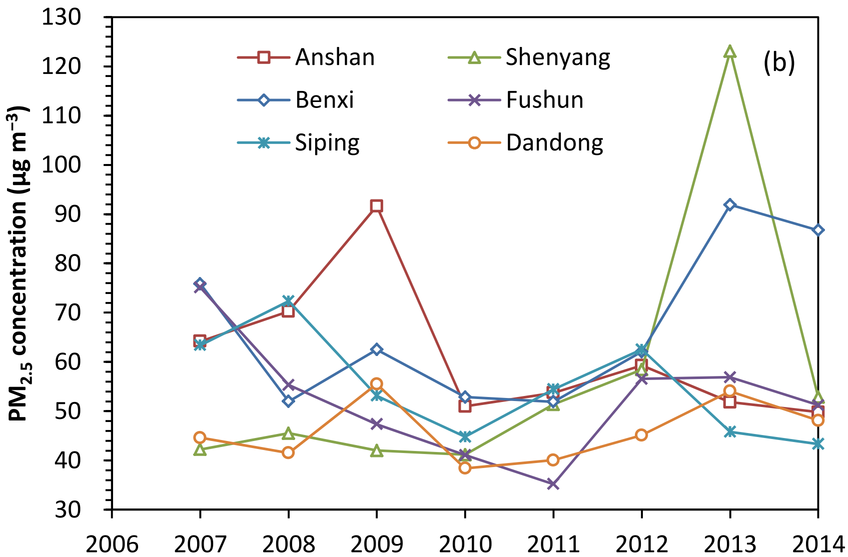

Anshan
Shenyang
Benxi
Fushun
Siping
Dandong
(b)
PM2.5 concentration (µg m−3)
130
120
110
100
90
80
70
60
50
40
30
2006
2007
2008
2009
2010
2011
2012
2013
2014

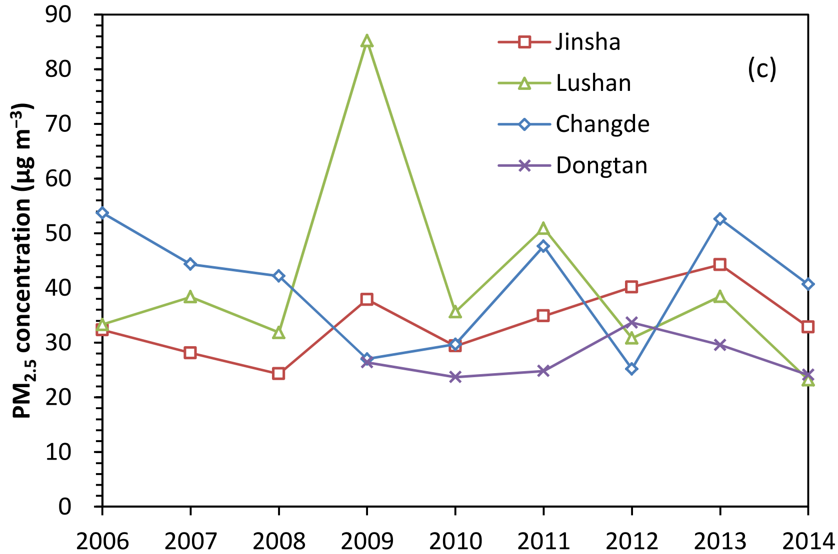

Jinsha
Lushan
Changde
Dongtan
(c)
PM2.5 concentration (µg m−3)
90
80
70
60
50
40
30
20
10
0
2006
2007
2008
2009
2010
2011
2012
2013
2014

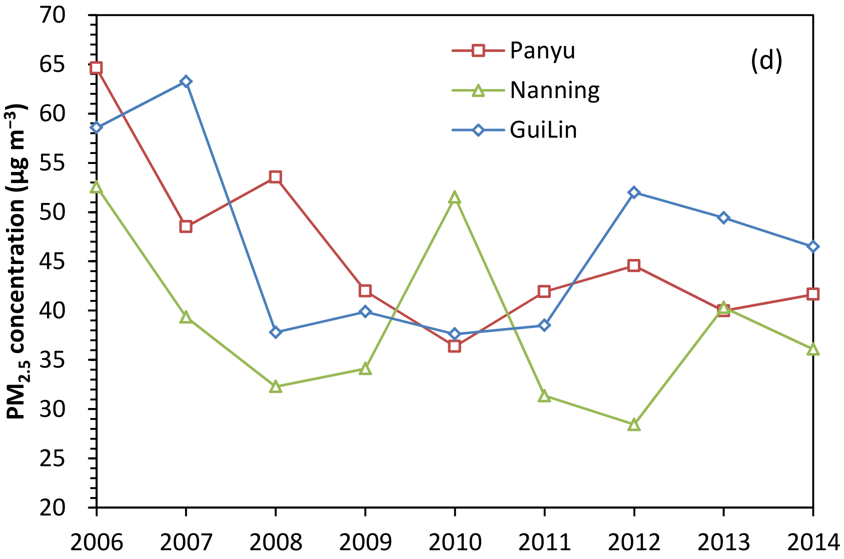

Figure 5. Interannual variations of $PM_{2.5}$ concentrations at the stations (a) on the HBP and Guanzhong Plain, (b) in northeast China, (c) along the middle and lower reaches of the Yangtze River, and (d) in southern China.

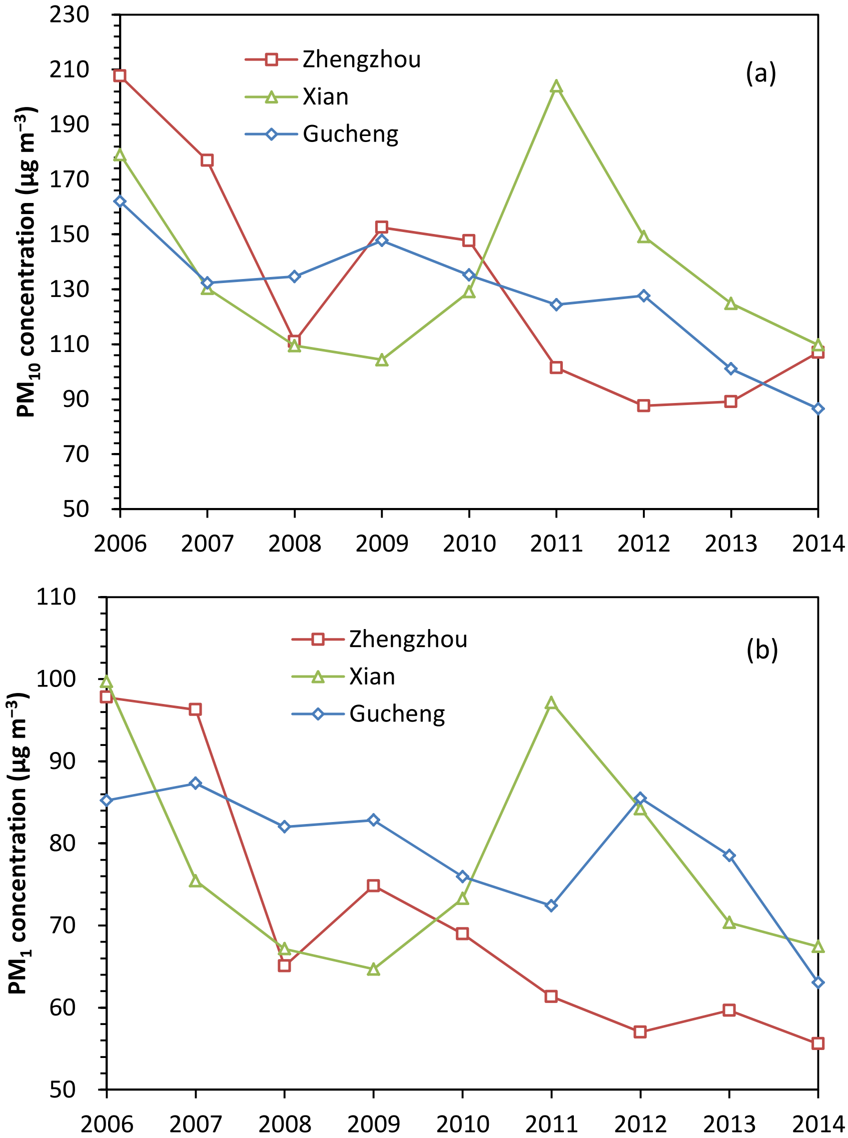

Figure 6. Interannual variation of (a) PM_{10} concentration and (b) PM_1 concentration at Zhengzhou, Xian and Gucheng.

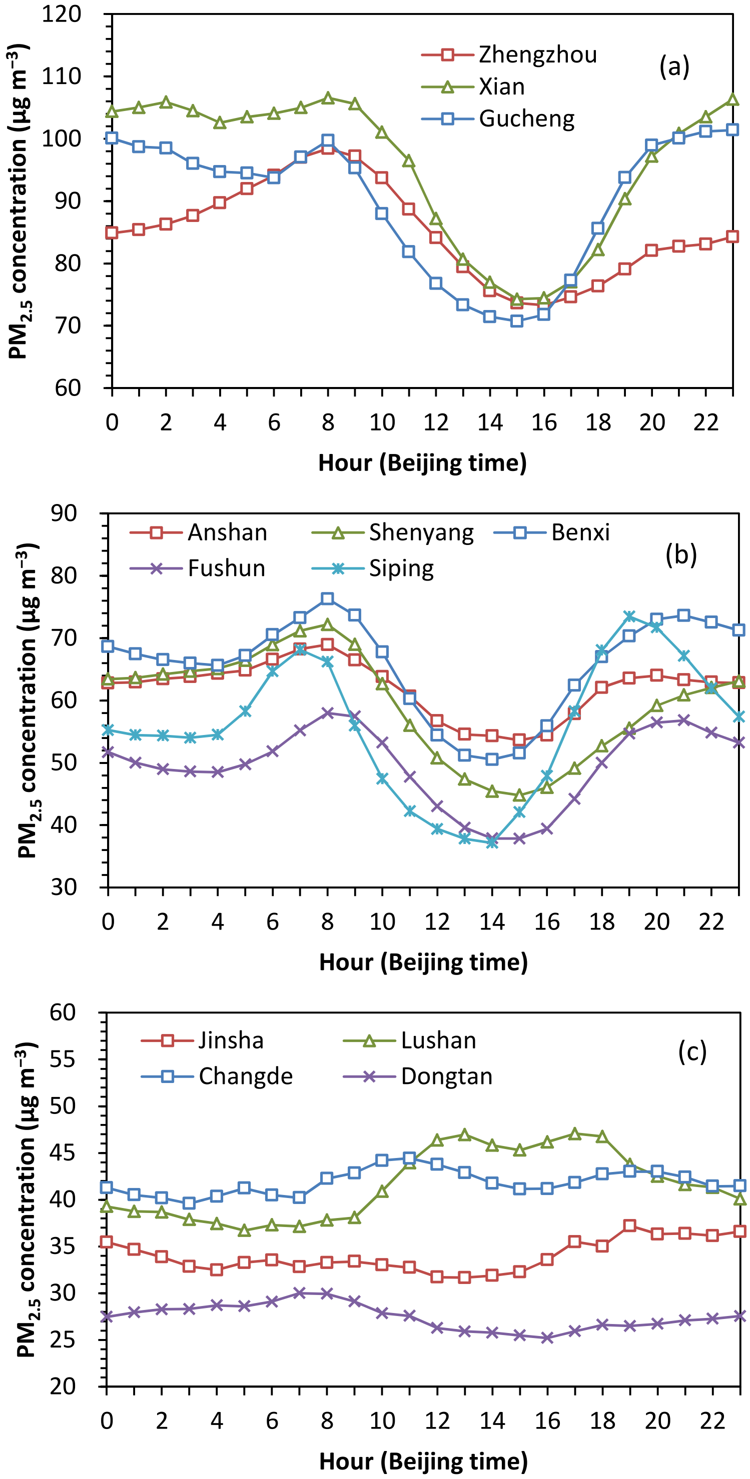

(a)
Zhengzhou
Xian
Gucheng
PM2.5 concentration (μg m−3)
Hour (Beijing time)
(b)
Anshan
Shenyang
Benxi
Fushun
Siping
PM2.5 concentration (μg m−3)
Hour (Beijing time)
(c)
Jinsha
Lushan
Changde
Dongtan
PM2.5 concentration (μg m−3)
Hour (Beijing time)

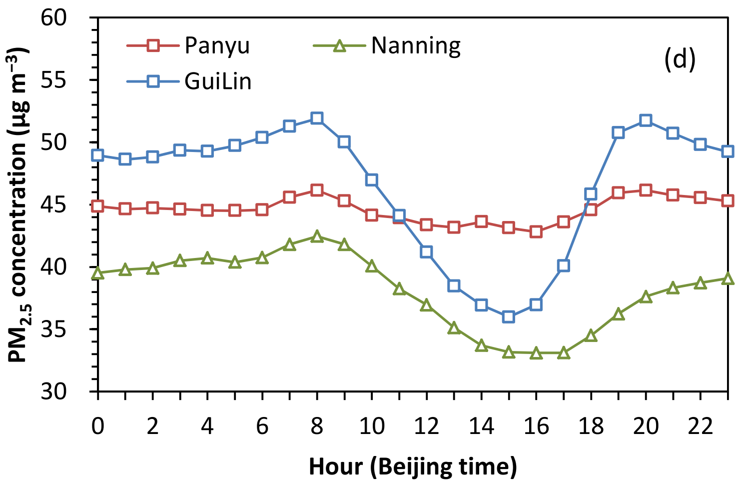

Figure 7. Diurnal variation of $PM_{2.5}$ concentrations at the stations (a) on the HBP and Guanzhong Plain, (b) in northeast China, (c) along the middle and lower reaches of the Yangtze River, and (d) in southern China.

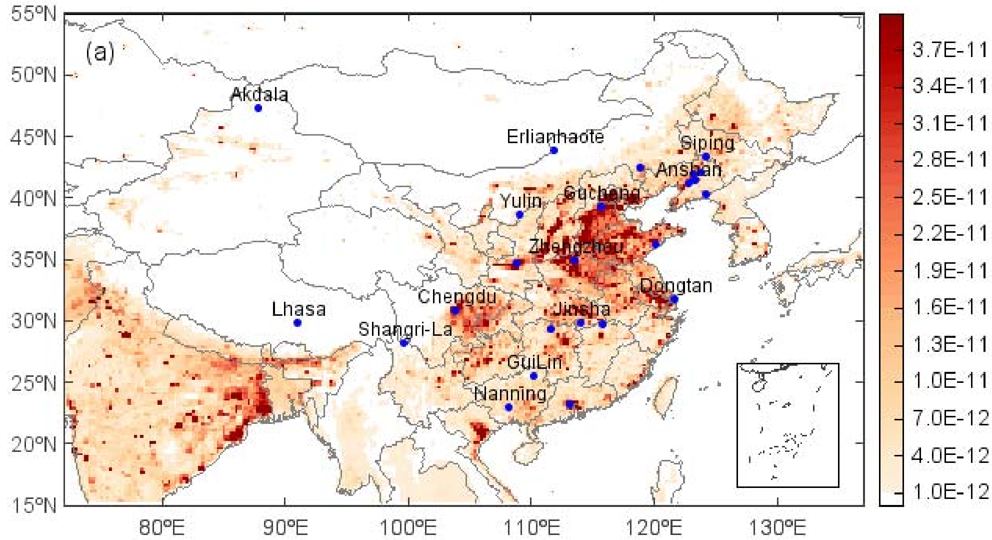
(a)
Akdala
Erlianhaote
Siping
Anshan
Yulin
Gucheng
Zhengzhou
Dongtan
Chengdu
Lhasa
Jinsha
Shangri-La
GuiLin
Nanning
55ºN
50ºN
45ºN
40ºN
35ºN
30ºN
25ºN
20ºN
15ºN
80ºE
90ºE
100ºE
110ºE
120ºE
130ºE
3.7E-11
3.4E-11
3.1E-11
2.8E-11
2.5E-11
2.2E-11
1.9E-11
1.6E-11
1.3E-11
1.0E-11
7.0E-12
4.0E-12
1.0E-12

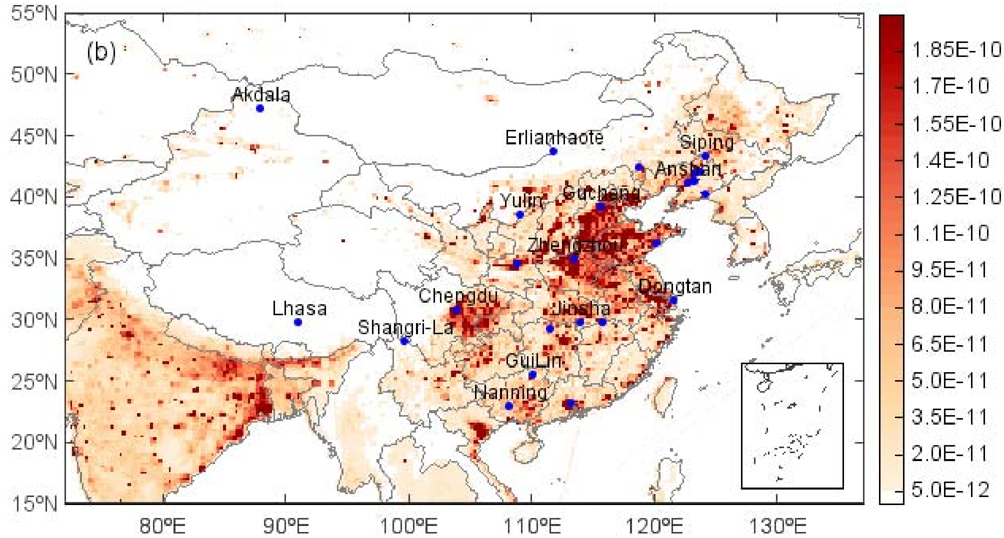
(b)
Akdala
Erlianhaote
Siping
Anshan
Yulin
Gucheng
Zhengzhou
Dongtan
Chengdu
Lhasa
Jinsha
Shangri-La
GuiLin
Nanning
55ºN
50ºN
45ºN
40ºN
35ºN
30ºN
25ºN
20ºN
15ºN
80ºE
90ºE
100ºE
110ºE
120ºE
130ºE
1.85E-10
1.7E-10
1.55E-10
1.4E-10
1.25E-10
1.1E-10
9.5E-11
8.0E-11
6.5E-11
5.0E-11
3.5E-11
2.0E-11
5.0E-12

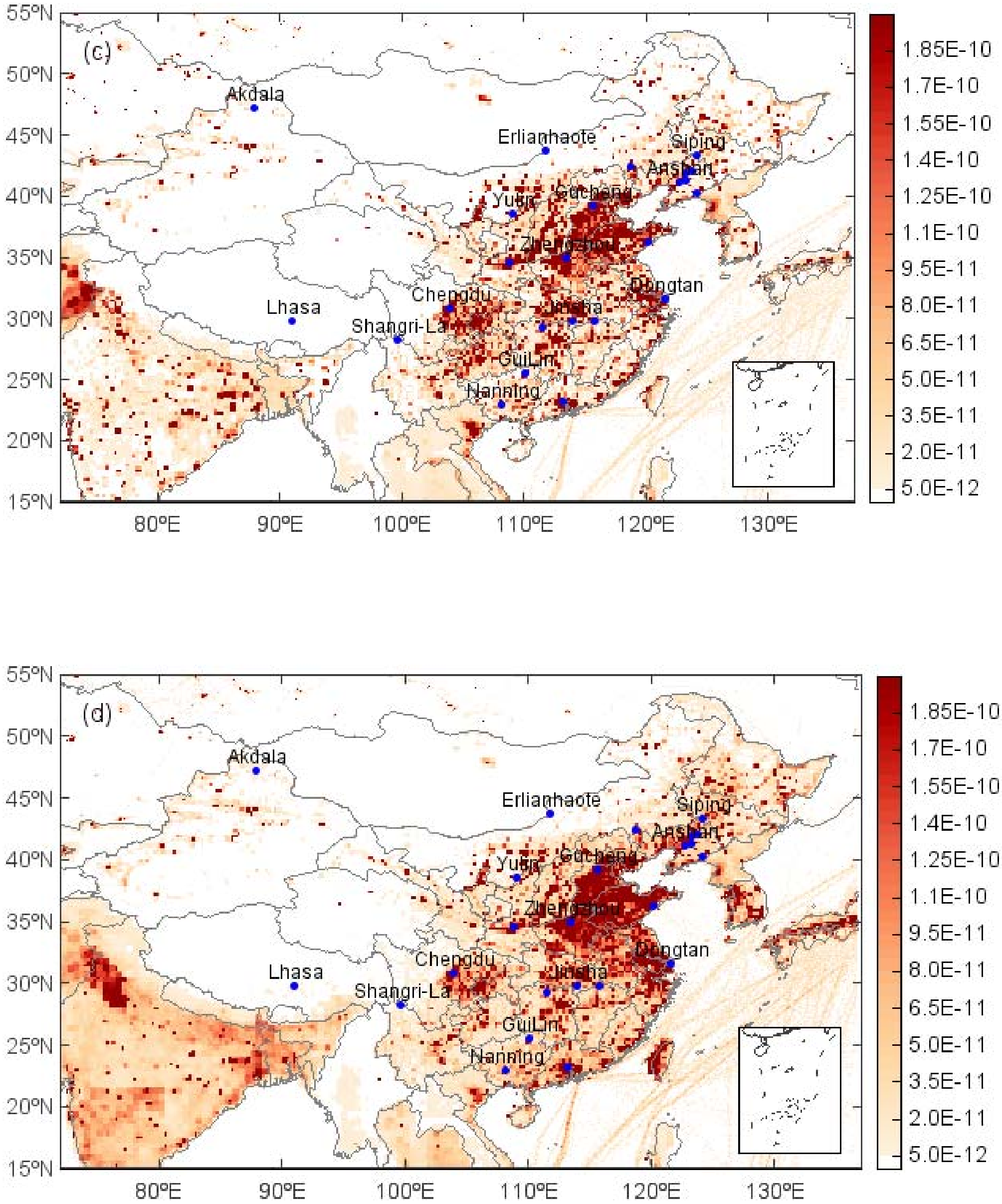

Figure 8. Anthropogenic emission distributions at a resolution of 0.1° × 0.1°, based on HTAP_v2 dataset: (a) BC; (b) $PM_{2.5}$; (c) SO_2; (d) NOx (units: kg m^{-2} s^{-2}).

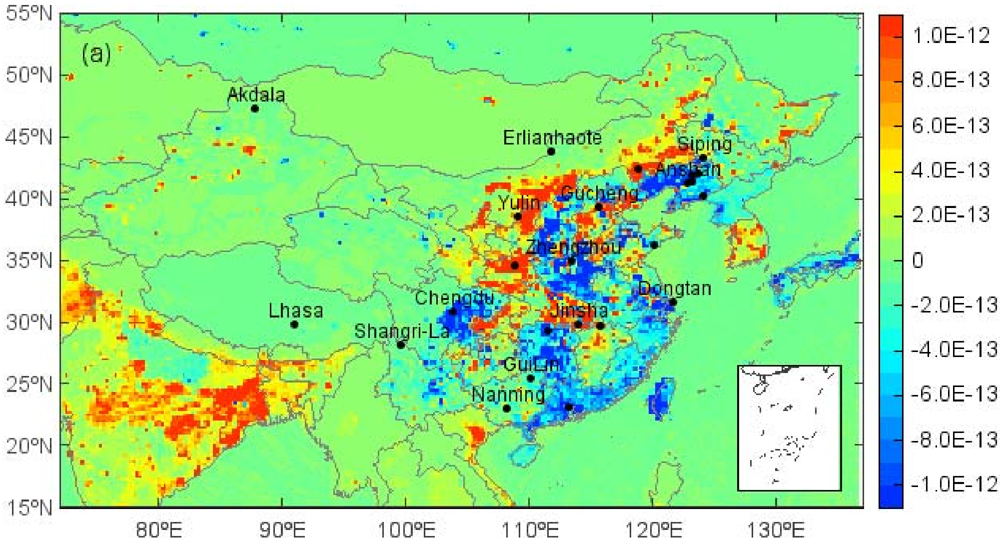
(a)
Akdala
Erlianhaote
Siping
Anshan
Yulin
Gucheng
Zhengzhou
Dongtan
Chengdu
Jinsha
Lhasa
Shangri-La
GuiLin
Nanning
55ºN
50ºN
45ºN
40ºN
35ºN
30ºN
25ºN
20ºN
15ºN
80ºE
90ºE
100ºE
110ºE
120ºE
130ºE
1.0E-12
8.0E-13
6.0E-13
4.0E-13
2.0E-13
0
-2.0E-13
-4.0E-13
-6.0E-13
-8.0E-13
-1.0E-12

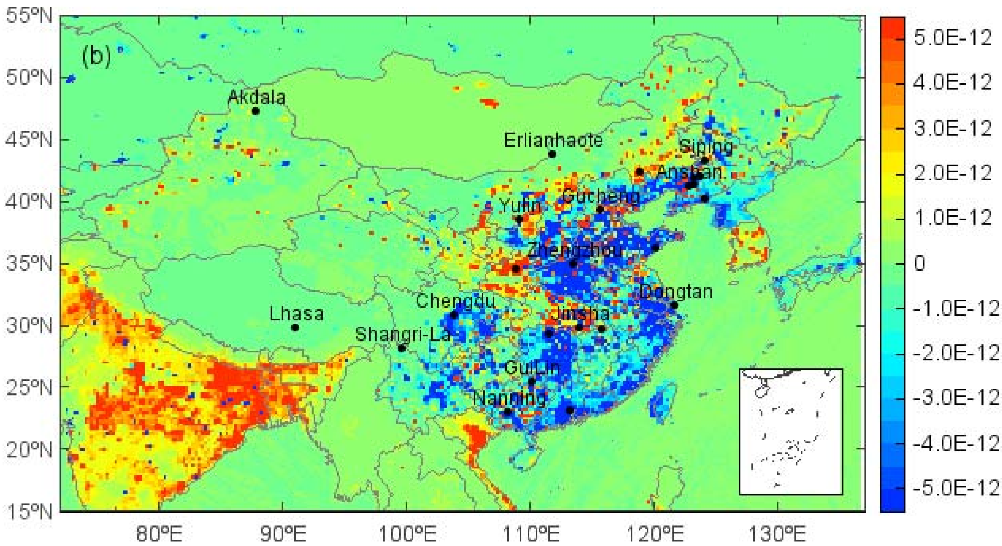
(b)
Akdala
Erlianhaote
Siping
Anshan
Yulin
Gucheng
Zhengzhou
Dongtan
Chengdu
Jinsha
Lhasa
Shangri-La
GuiLin
Nanning
55ºN
50ºN
45ºN
40ºN
35ºN
30ºN
25ºN
20ºN
15ºN
80ºE
90ºE
100ºE
110ºE
120ºE
130ºE
5.0E-12
4.0E-12
3.0E-12
2.0E-12
1.0E-12
0
-1.0E-12
-2.0E-12
-3.0E-12
-4.0E-12
-5.0E-12

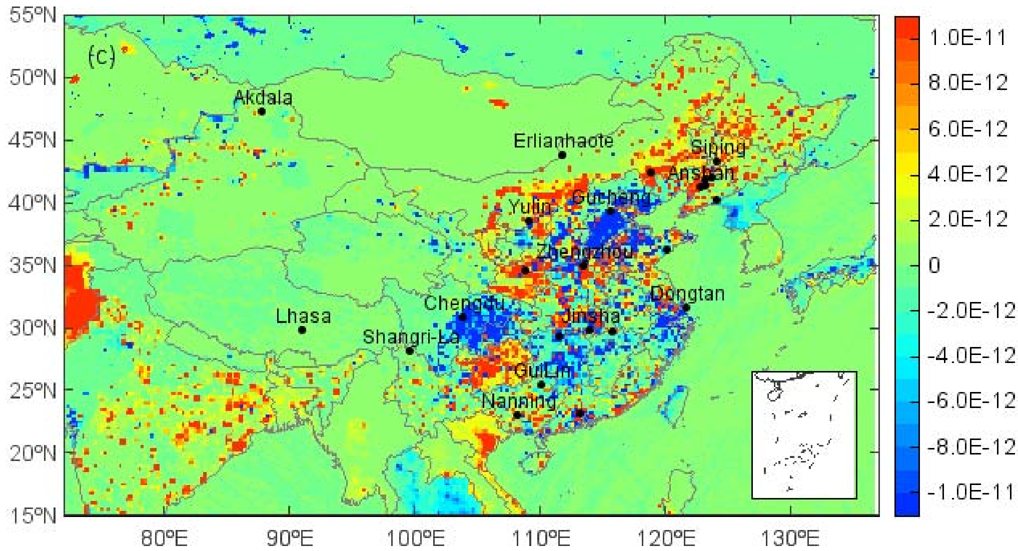

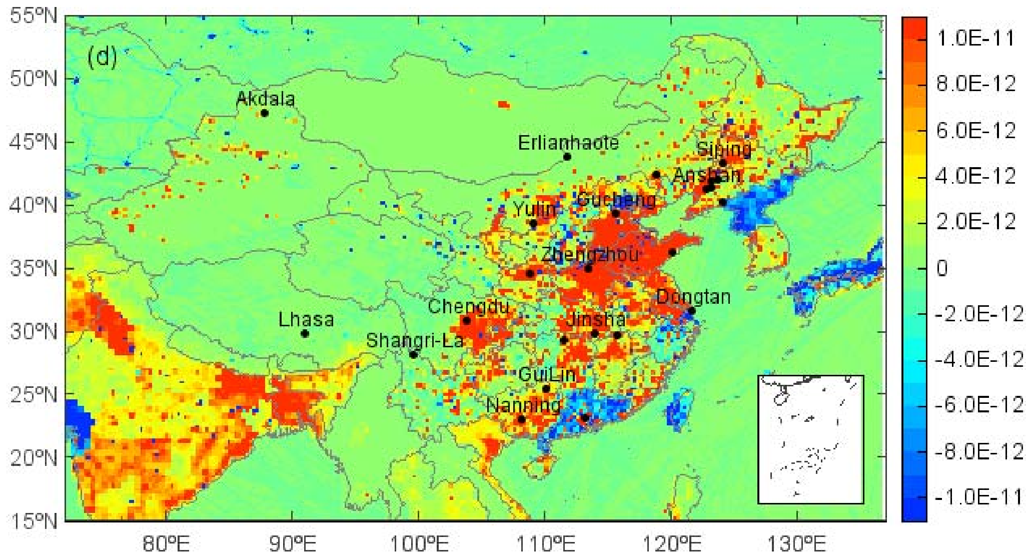

Figure 9. Emissions differences between 2010 and 2008 at a resolution of 0.1° × 0.1°, based on HTAP_v2 dataset: (a) BC; (b) $PM_{2.5}$; (c) SO_2; (d) NOx (units: kg m^{-2} s^{-2}).

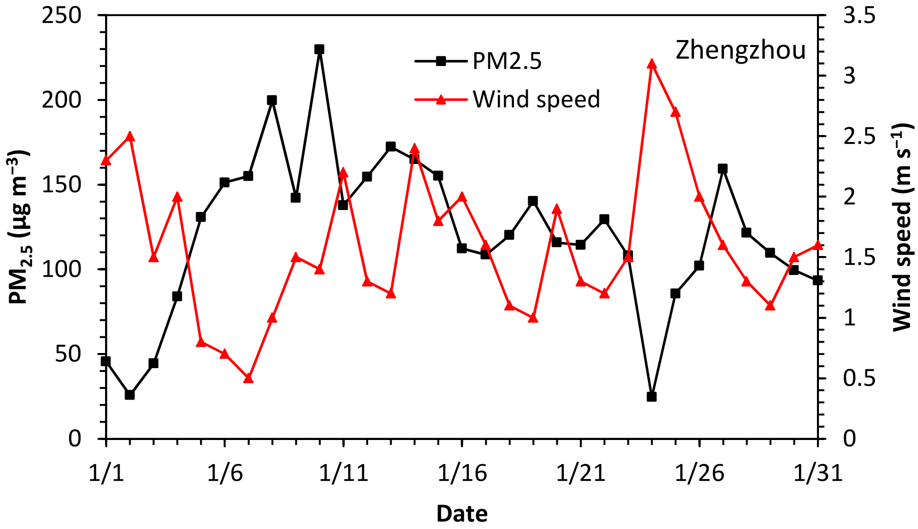

Zhengzhou
PM2.5
Wind speed
PM$_{2.5}$ (µg m^{-3})
Wind speed (m s^{-1})
Date

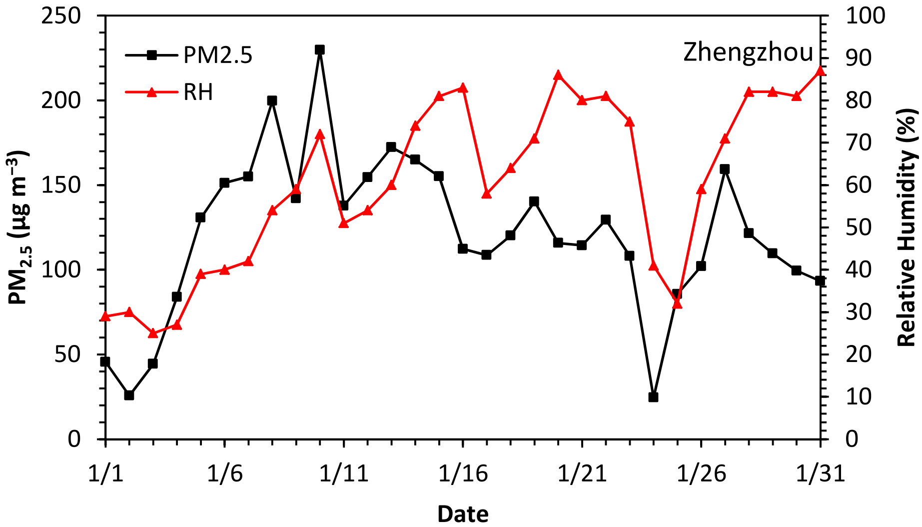

Zhengzhou
PM2.5
RH
PM$_{2.5}$ (µg m^{-3})
Relative Humidity (%)
Date

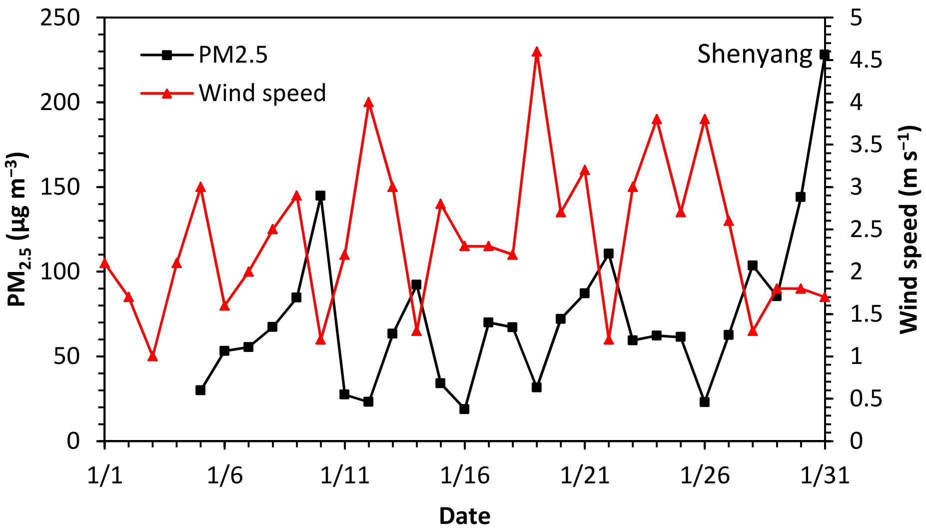

Shenyang
PM2.5
Wind speed
PM$_{2.5}$ (µg m^{-3})
Wind speed (m s^{-1})
Date

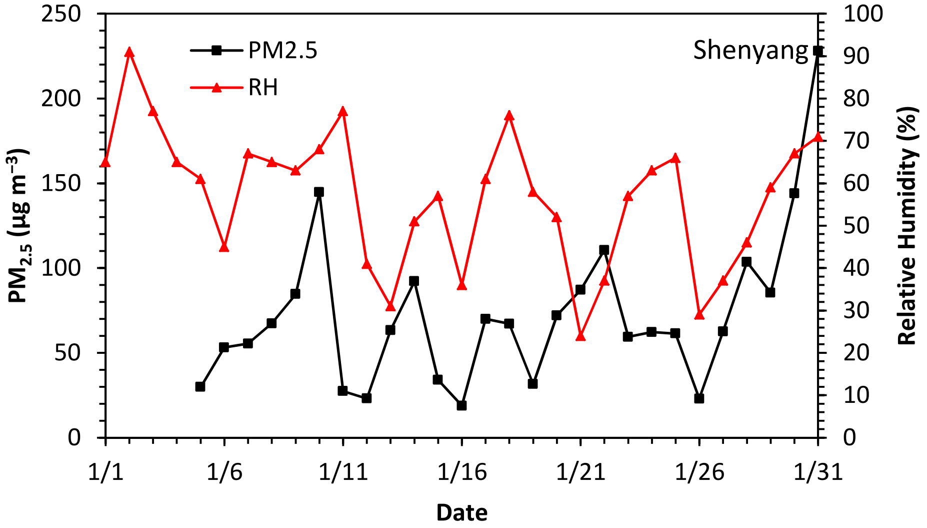

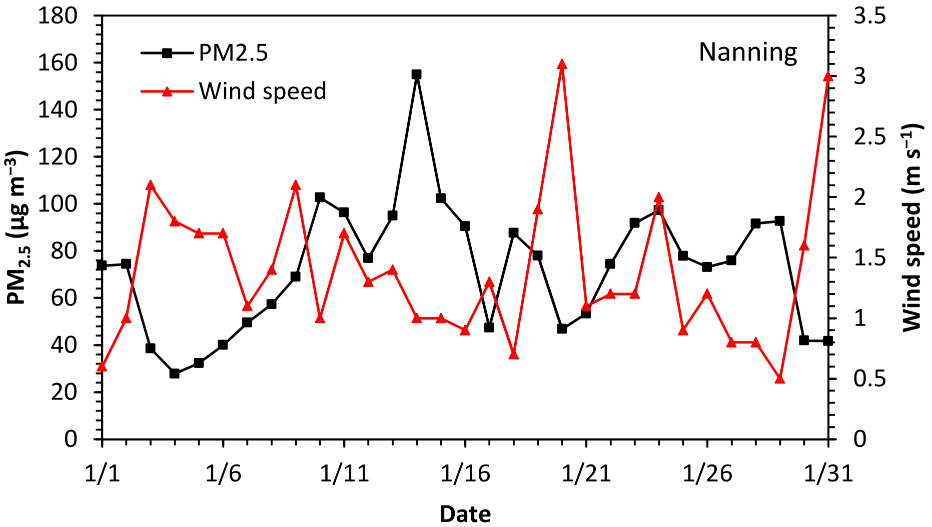

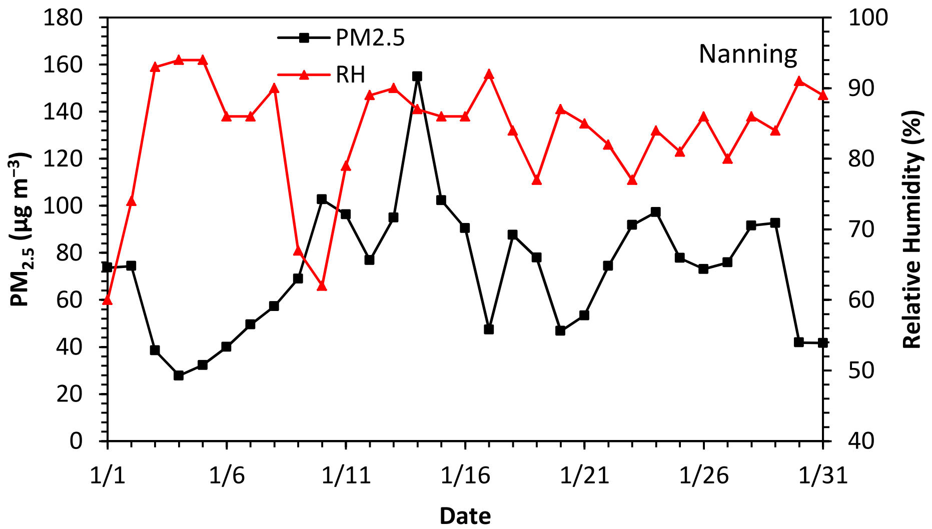

Figure 10. Daily averaged $PM_{2.5}$ concentrations vs wind speed and relative humidity at Zhengzhou, Shenyang and Nanning in January 2013.

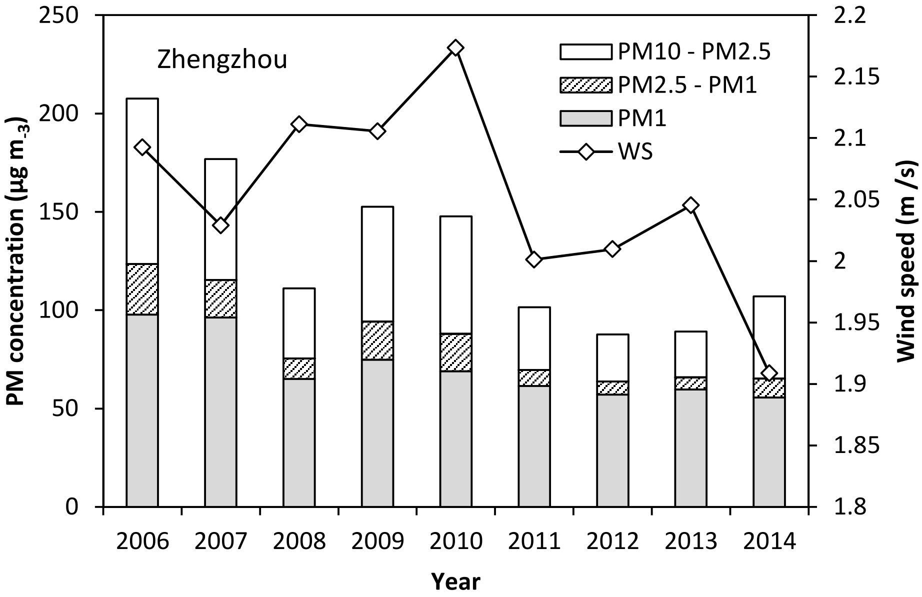
Zhengzhou
PM10 - PM2.5
PM2.5 - PM1
PM1
WS
PM concentration (µg m-3)
Wind speed (m /s)
Year
0
50
100
150
200
250
1.8
1.85
1.9
1.95
2
2.05
2.1
2.15
2.2
2006
2007
2008
2009
2010
2011
2012
2013
2014

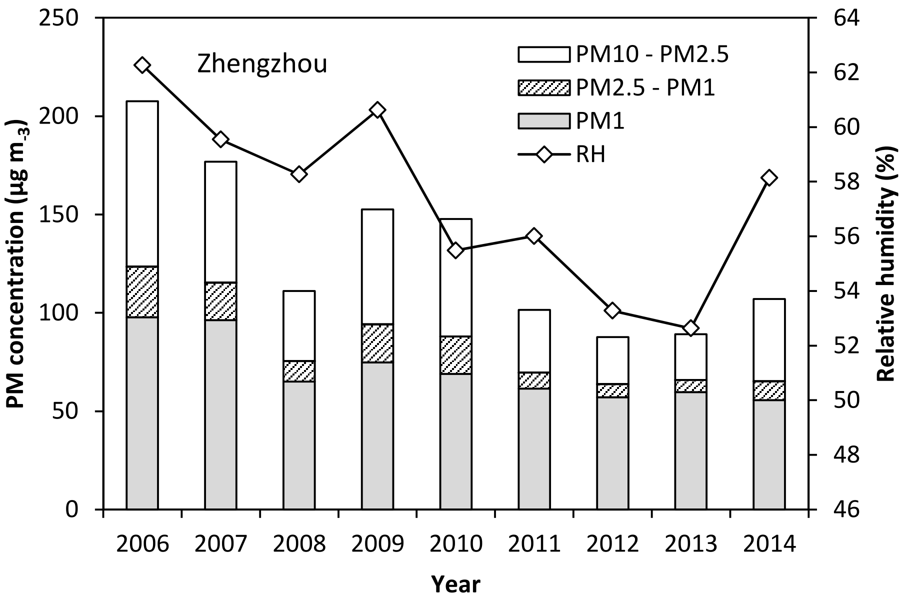
Zhengzhou
PM10 - PM2.5
PM2.5 - PM1
PM1
RH
PM concentration (µg m-3)
Relative humidity (%)
Year
0
50
100
150
200
250
46
48
50
52
54
56
58
60
62
64
2006
2007
2008
2009
2010
2011
2012
2013
2014

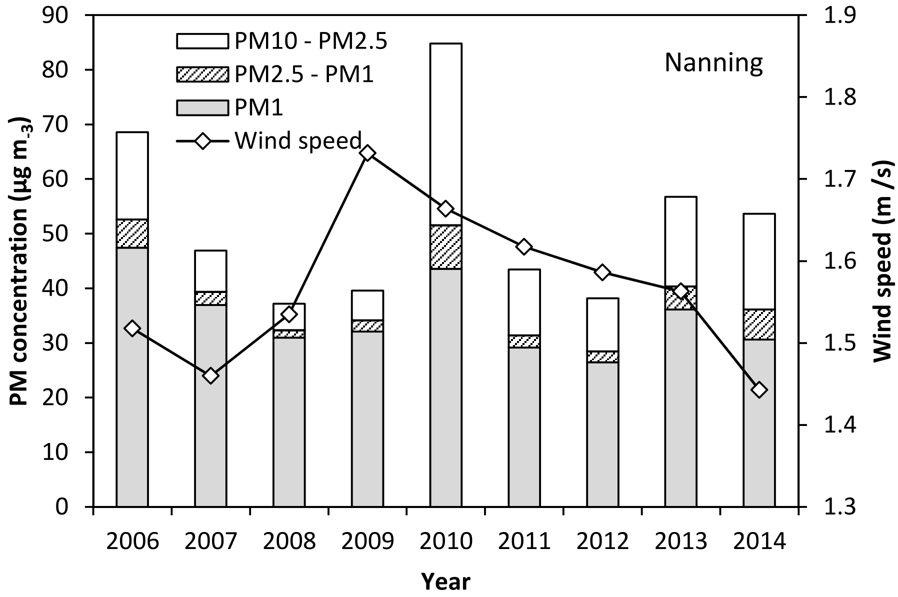

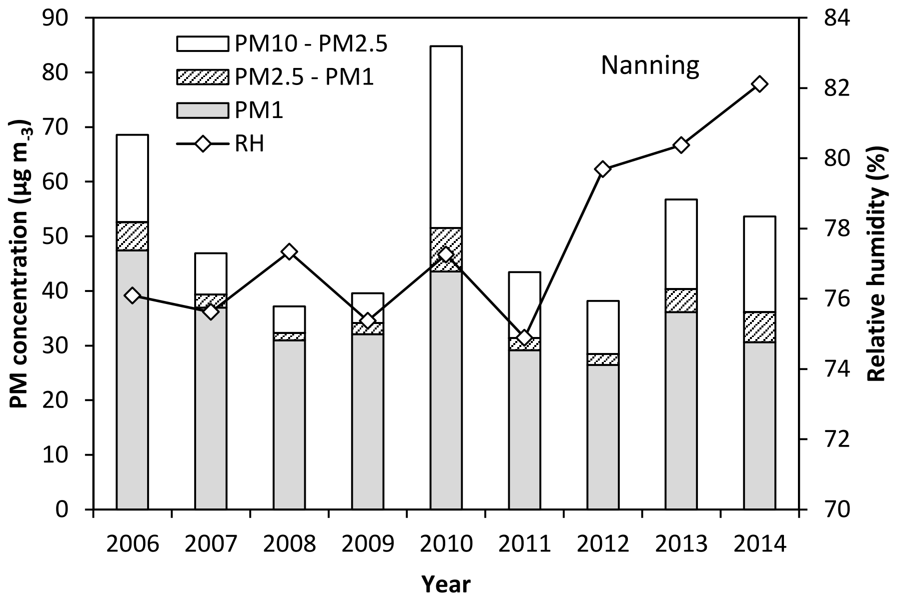

Figure 11. Interannual variation of PM_{10}, $PM_{2.5}$ and PM_1 vs wind speed and relative humidity at Zhengzhou and Nanning.